Bulletin of the Earthquake
Research Institute
Vol. 40 (1962), pp. 1-65

1. *The Westward Drift of the Magnetic Field of the Earth*.*

By Takesi Yukutake,†

Graduate School, University of Tokyo.

(Read Nov. 28, 1961.—Received Dec. 27, 1961.)

Contents

Summary

Secular variations in the geomagnetic field are studied with the intention of making a clear-cut separation of the variation due to

* Communicated by T. Rikitake

† Present address; Earthquake Research Institute.

the westward drift of the non-dipole field from that due to the growth and decay of the said field. By making use of a few different methods, the most probable velocity of the westward drift is determined as 0.20°/*year* on average. It turns out that the major parts of the observed field variation are caused by the drift. It is not reasonable, however, to ignore the residual variation in the field which cannot be explained by the drift. Growth and decay in the non-dipole field seems to be responsible for the residual field. The field variation in historical time is also likely to be approximately accounted for by the drift, so that it is suggested that the non-dipole field has a life-time as long as several hundred years or more.

Introduction.

The secular variation in the earth's magnetic field has long been one of the most elusive problems in geophysics. As the magnetic compass had been in use in navigation since the 11th or 12th century, it has been a matter of practical importance for sailors to know the direction of the magnetic meridian on the sea. Since the 16th century, measurements of the direction of the earth's magnetic field at many places have brought out the world's distribution of the direction of the magnetic meridian or declination in fair detail. The distribution of other geomagnetic elements have become clear as well. At the same time, it has turned out that the geomagnetic field continually undergoes gradual changes. Being called the secular variation, changes of this sort have been investigated by numerous workers with the intention of arriving at some information about the earth's interior through an analysis of these changes. Unfortunately, however, it cannot be said that anything absolutely certain as to the cause of the secular variation has been brought forth by now.

Some authors have classified the variations observed in the field into a few types of similar nature and speculated on the likely causes of the variations taking place in the earth[1]. Meanwhile, many authors have studied time-changes in the spherical harmonic coefficients obtained by spherical harmonic analyses of the earth's magnetic field.

Since the beginning of this century, it has become customary to chart maps of the rate of change in the field, called charts of the "secular" variation, by calculating the differences in the field between two epochs of ten year intervals. These distributions of secular varia-

1) C. GAIBAR-PUERTAS, *Observ. del. Ebro, Memo. No.* **11** (1953).

tions thus compiled generally resemble those of the non-dipole part of the earth's field so closely that many authors have considered that the rate of change observed could be mostly explained as being that of the non-dipole field. Taking into account the rapid rate of change sometimes observed, sources of the secular variation have been surmised to lie in the top-layer of the core of the earth. Should something deep in the core be responsible for secular variation, the highly conducting core would shield such rapid variation in the magnetic field so strongly that no change could emerge through the core's surface. It has been believed that the non-dipole field might perhaps be caused by eddy currents near the surface of the core and changes in their intensity might be observed as secular variations[2),3),4),5)]. McNish[6)] approximated the non-dipole field by 14 dipoles in radial direction near the surface of the core. Lowes and Runcorn[2)] also attempted to explain the observed rate of change by time-dependent dipoles at the surface of the core. McDonald[7)] considered a local pattern of the rate of change in the field with a special distribution as being the sources of the variation and approximated the observed rate of change in the world by scattering those special patterns at the core boundary.

On the other hand, the westerly movement of the geomagnetic field has been noticed since historical time. Bauer studied the westerly drift of the line of zero declination tracing it back to the middle of the sixteenth century and obtained the mean velocity of $0.22°/yr$. Carlheim-Gyllensköld noticed a marked westerly drift of a few terms of spherical harmonic analyses of the goemagnetic field. More detailed and quantitative analyses were carried out by Bullard and others[8)]. Constructing the maps of the non-dipole field at epochs 1907.5 and 1945, they determined the most probable shift of the magnetic field during this period. The most likely value for the drift velocity obtained by them is $0.18°/yr$. Whitham[9)] examined the drift velocity in Canada by making use of detailed magnetic maps and found no

2) F. J. LOWES and S K. RUNCORN, *Phil. Trans. Roy. Soc. London, A,* **243** (1951), 525.

3) W. M. ELSASSER, *Rev. Mod. Phys.*, **22** (1950), 1.

4) W. M. ELSASSER, *Amer. Jour. Phys.*, **23** (1955), 590.

5) W. M. ELSASSER, *Amer. Jour. Phys.*, **24** (1956), 85.

6) A. G. MCNISH, *Trans. Amer. Geophys. Un.*, **21** (1940), 287.

7) K. L. MCDONALD, *Jour. Geophys. Res.*, **60** (1955). 377.

8) E. C. BULLARD, C. FREEDMAN, H. GELLMAN and J. NIXON, *Phil. Trans. Roy. Soc. London,* **243** (1950), 67.

marked tendency of drift there. He surmised that there should be a large local fluctuation in the westward drift in Canada in contrast to the drift on the world-wide scale.

The magnetic field observed at one observatory changes with time accordingly as the field drifts westwards. Therefore the observed variation should be partly caused by the drift. This has been previously noticed by Lowes[10] and Whitham[9]. Assuming dipoles at the core's surface as the sources of the non-dipole field, Lowes examined the contribution of the drift of these dipoles to the observed secular variation. He reached a conclusion that the drift may account for a large part of the secular variation actually observed. Whitham estimated the drift velocity so as to make the contribution of the drift to the observed rate a maximum. Recently Nagata and Rikitake[11] made the remark about the relation between the observed rate of change and the non-dipole field that the foci of the isopors for secular variation seemed to exist in general to the west of the centres of the non-dipole field. This may suggest that the rates of change observed are affected by the westward drift of the magnetic field.

Although the existence of the westward drift of the earth's field seems to be an established fact, there are many things awaiting further investigation in more detail, *i.e.*, whether or not the drift velocity varies systematically along parallel circles or along meridians, whether or not the field of different extent drifts with the same velocity and so on. It has not been estimated what percentage of the secular variation may be attributed to the drift. The writer attempts here to investigate these points as closely as possible with the data available at present.

Chapter 1. Two Causes of Geomagnetic Secular Variation Observed on the Earth's Surface.

In the earth's core, it is widely believed, on the basis of the dynamo theory of the main geomagnetic field, that a strong toroidal field is in existence. If there are irregular fluid motions in the core, the interactions between the motions and the toroidal field, as well as the dipole field, would induce some electric currents which in turn would produce irregular magnetic fields of smaller scale. It is likely that a large

9) K. WHITHAM, *Canad. Jour. Phys.*, **36** (1958), 1372.
10) F. J. LOWES, *Ann. Geophys.*, **11** (1955), 91.
11) T. NAGATA and T. RIKITAKE, *Jour. Geomag. Geoele., Kyoto*, **9** (1957) 42.

portion of the time-dependent fields induced by such a mechanism in the deep part of the core is shielded by the highly conducting layer of the core, so that only the time-variation in the magnetic field, taking place in the very shallow part of the core, can be observed on the earth's surface. The irregular fields that are customarily called the "non-dipole part of the geomagnetic field" have been therefore accepted by most geomagneticians as the products of the turbulent motion near the core boundary. And it has been also tacitly taken for granted that the secular variation observed is mainly caused by the growth and decay of these turbulences. Such a view is exactly correct, if the whole core be firmly coupled to the mantle and rotating with the same angular velocity as that of the mantle. However, when there exists a slip between the core and the mantle, the situation becomes different. Even if there be no change in the magnetic field at the surface of the core, the rotation of the magnetic field relative to the mantle will cause some changes in the magnetic field which can be noticed by an observer fixed to a point on the earth's surface. If a hill or a dale of a field distribution originating in the core passes through an observatory with a certain speed, for instance, we cannot discriminate it from a change in the intensity of a dipole situated beneath the observatory. Since it is well known that there is a tendency for the geomagnetic field to drift westwards, the contribution of such a westward drift to the secular variation observed seems to deserve more detailed analyses.

In a moving conductor such as the fluid in the earth's core, variation in the magnetic field $\boldsymbol{H}$ satisfies the following induction equation (in *e. m. u.*).

$$\frac{\partial \boldsymbol{H}}{\partial t}=\frac{1}{4\pi\kappa}\nabla^2\boldsymbol{H}+\mathrm{curl}\ (\boldsymbol{v}\times\boldsymbol{H})$$

where $\boldsymbol{v}$ is the local velocity of the conducting fluid and κ represents the electrical conductivity. This equation can be rewritten as follows

$$\frac{\partial \boldsymbol{H}}{\partial t}=\frac{1}{4\pi\kappa}\nabla^2\boldsymbol{H}-(\boldsymbol{v}\cdot\nabla)\boldsymbol{H}+(\boldsymbol{H}\cdot\nabla)\boldsymbol{v}. \qquad (1\text{–}1)$$

The first term on the righthand-side represents the field dissipation due to Joule heating. The second term is the variation caused by the convection of the field by the fluid motion. The last term means that the magnetic field is strengthened by stretching the lines of force. The variation observed on the earth's surface is a superposition of

changes due to all of these causes. Referring to the steadily rotating mantle, we shall denote the westerly drift velocity by v_0, and the fluid motion superposing on it by v_1. Then we can write the equation (1-1) in the following form.

$$\frac{\partial \boldsymbol{H}}{\partial t}=\frac{1}{4\pi\kappa}\nabla^2\boldsymbol{H}-(\boldsymbol{v}_0\cdot\nabla)\boldsymbol{H}+(\boldsymbol{H}\cdot\nabla)\boldsymbol{v}_0-(\boldsymbol{v}_1\cdot\nabla)\boldsymbol{H}+(\boldsymbol{H}\cdot\nabla)\boldsymbol{v}_1. \qquad (1\text{-}2)$$

The second term on the righthand-side is the variation due to the westerly rotation of the magnetic field. If the drift velocity v_0 had been well determined, the variation caused by other causes could be estimated from the above equation. However, v_0 estimated so far indicates a variety accordingly as the data used or the methods adopted differ. Bullard and others[12] obtained a value of $0.18°/yr$ from comparison of analyses of the non-dipole field at two epochs 1917.5 and 1945. Repeating the same procedure, for the rate of change in the field they obtained $0.32°/yr$. From the data of the non-dipole field and its secular variation in Canada, Whitham[13] made a similar analysis. He obtained values of $0.056°/yr$ W and $0.00°/yr$ W respectively. Vestine's study[14] on the drift of the eccentric dipole indicated that it had been moving westwards with an average velocity of $0.29°/yr$ over more than one hundred years. Recently, Nagata and Syono[15] have studied secular variation, on the basis of new data, getting a value of about $0.2°/yr$ for the westward drift. In order to see why we had these diverse results, it is first intended in this paper to determine the velocity of the westward drift as well as its latitudinal and longitudinal dependency as accurately as possible by making use of new methods of analysis.

From the equation (1-2), when the magnetic field is assumed to decay only by diffusion, we estimate the decay time in the magnetic field of several hundred kilometer extent to be about a few thousand years. It remains uncertain, however, whether or not the irregular field may disappear within this period, because we have no accurate information about the velocity field v_1 which may destroy or intensify the complicated magnetic field. There seems to be no means of presuming the relative importance of various terms in equation (1-2), so

12) E. C. BULLARD *et al*, *loc. cit.*, 8).
13) K. WHITHAM, *loc. cit.*, 9).
14) E. H. VESTINE, *Jour. Geophys. Res.*, **58** (1953), 127.
15) T. NAGATA and Y. SYONO, *Jour. Geomag. Geoele. Kyoto*, **12** (1961) 84.

that we shall first assume that the observed secular variation is mainly caused by the westward drift of the magnetic field, that is, the second term is the most important. Equation (1–2) can also be written in the following form.

$$\frac{\partial \boldsymbol{H}}{\partial t}+(\boldsymbol{v}_0\cdot\nabla)\boldsymbol{H}=\frac{1}{4\pi\kappa}\nabla^2\boldsymbol{H}+(\boldsymbol{H}\cdot\nabla)\boldsymbol{v}_0-(\boldsymbol{v}_1\cdot\nabla)\boldsymbol{H}+(\boldsymbol{H}\cdot\nabla)\boldsymbol{v}_1 \qquad (1\text{–}3)$$

This equation is only valid in the core. In the earth's mantle or on the surface of the earth, we have an equation of the same kind which governs the magnetic field. The equation is

$$\frac{\partial \boldsymbol{H}}{\partial t}+(\boldsymbol{v}_0'\cdot\nabla)\boldsymbol{H}=\boldsymbol{R}(t,\boldsymbol{r}) \qquad (1\text{–}4)$$

where $\boldsymbol{r}$ denotes the positional vector and $\boldsymbol{v}_0'$ is the drift velocity of the field in the mantle. It coincides with the velocity in the core only in the case that the mantle has no electric conductivity or that the phenomenon is steady with time. $\boldsymbol{R}(t, \boldsymbol{r})$ is the residual field after the variation due to the westward drift has been subtracted from the observed time-variation $\partial\boldsymbol{H}/\partial t$, and it enables us to estimate the field variation actually taking place in the earth's core as described by the righthand-side of equation (1–3). If we have knowledge on the rate of change $\partial\boldsymbol{H}/\partial t$ and the field distribution $\boldsymbol{H}$, we are able to adjust the velocity $\boldsymbol{v}_0$ so as to minimize the residual field variation R. There are two ways of minimizing R. One is to rely on the least square method, integrating the square of the residual R over a sufficient interval of time. Another is to integrate it over an extensive area in space. That is

$$\left.\begin{aligned}&\text{(A)}\quad \Phi=\int[R(t,\boldsymbol{r})]^2dt\\&\text{(B)}\quad \Phi=\int[R(t,\boldsymbol{r})]^2ds\end{aligned}\right\} \qquad (1\text{–}5)$$

If R should vary at random with time or in space, the velocity thus determined could safely be regarded as the velocity with which the magnetic field moves over the specified period or the spatial extent considered.

Most of the analyses so far made are based on the latter method. Bullard and others took the differences between the non-dipole field in longitude ϕ in 1945, $H_{1945}(\phi)$, and that in 1907.5 shifted D degrees to

the west. $H_{1907.5}(\phi+D)$ *i.e.*

$$\varepsilon=H_{1945}(\phi)-H_{1907.5}(\phi+D)\ .$$

They computed the summation $\sum\varepsilon^2$ along the *circle of latitude*, and determined the most probable shift D along that latitude circle by making $\sum\varepsilon^2$ a minimum. When the shift D is small, we can write

$$H_{1907.5}(\phi+D)=H_{1907.5}(\phi)+D\frac{\partial H_{1907.5}(\phi)}{\partial\phi}. \qquad (1\text{–}6)$$

Substituting this into the equation given before, we have

$$\varepsilon=[H_{1945}(\phi)-H_{1907.5}(\phi)]-D\frac{\partial H_{1907.5}(\phi)}{\partial\phi}. \qquad (1\text{–}7)$$

This is an integrated form of the equation (1–4). Correlating the magnetic potential of the main field at one epoch to that of the rate of change in the field at the same epoch, Whitham obtained the drift velocities of harmonic constituents. This procedure also contains a process of summation along latitude circles. Recently Nagata and Syono draw a histogram of the drift velocity of spherical harmonics after a calculation similar to Whitham's one. This also belongs to the second method in our classification.

The above-mentioned methods of determining the velocity work satufactorily only in the cases in which the residuals **R** are small and can easily be ruled out by their integration over a wide range of time or space. When **R** is large, or when the variation caused by the irregular complicated flow of fluid is more predominant than that due to the simple drift, it would be natural that we obtain greatly scattered values of velocity for different epochs and different data. If the velocities scatter in a wide range, it may be supposed that the growth and decay of the turbulent field are taking place rather rapidly. On the other hand, if the velocities determined for different epochs agree approximately with one another, we may take the velocity as the true one. In that case it may be allowable to conclude that the secular variation treated in the analyses is mainly caused by the general flow of the magnetic field.

Chapter 2. Westward Drift of Magnetic Potential.

Spherical harmonic analysis is pherhaps one of the most convenient ways of representing the general features of the earth's magnetic field.

By means of spherical harmonic analysis, we can resolve a complicated field into spherical harmonic constituents of various degrees and orders. Since such a procedure is made only for mathematical convenience, however, it is doubtful that every harmonic constituent derived from the analysis has a physical meaning. Attention should be paid to this point especially in the study of the time variation of the magnetic field. In this chapter, the writer is going to make use of the results of the spherical harmonic analyses hitherto made in order to examine further the property of the drift velocity in the hope of clarifying its characteristics in relation to space and time.

2–1. Phase shift with time.

Bullard and others[16] examined the drift in the harmonic constituents and obtained a remarkable result of their drifting westwards. In the light of the discussion in the beginning of this chapter, however, it will not be possible to put much significance on the differences in the velocities between different constituents. It would be desirable to deal with the distribution of the magnetic field in its original form as far as possible. What the writer is going to do in this section is to expand the magnetic field in a form of the Fourier series along a certain latitude circle. After that, the phase shift of their components is examined with regard to time.

Let V be the magnetic potential of the earth's field. Specifying a colatitude θ, we have

$$V=a\sum_{m}(G_m\cos m\lambda+H_m\sin m\lambda) \tag{2–1}$$

where a and λ denote the earth's radius and the geograghic longitude. G_m and H_m are defined by making use of the Gaussian constants ${g_n}^m$, ${h_n}^m$ in the following equations.

$$\left.\begin{aligned} G_m&=\sum_{n=m}\left(\frac{a}{r}\right)^{n+1}{g_n}^m{P_n}^m(\cos\theta)\\ H_m&=\sum_{n=m}\left(\frac{a}{r}\right)^{n+1}{h_n}^m{P_n}^m(\cos\theta)\end{aligned}\right\}. \tag{2–2}$$

The equation (2–1) gives the distribution of the magnetic potential along a certain circle of colatitude θ. It can be also written as follows.

16) E. C. BULLARD *et al*, *loc. cit.*, 8).

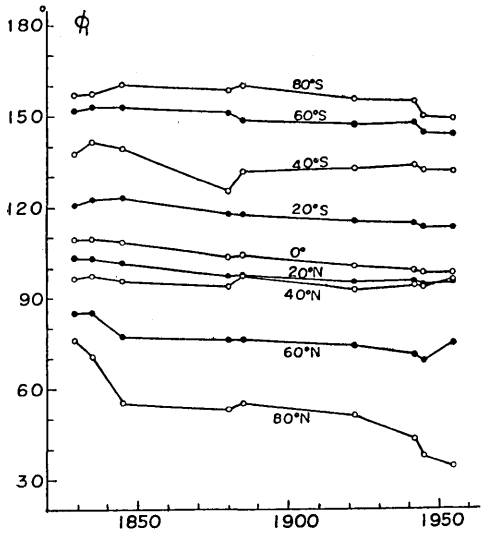

Fig. 2-1(a). ϕ_1 when the equatorial dipole is included.

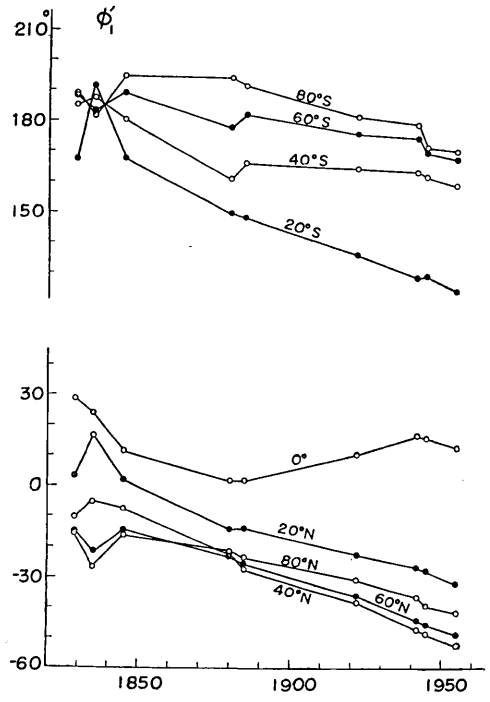

Fig. 2-1(b). ϕ_1' when the equatorial dipole is excluded.

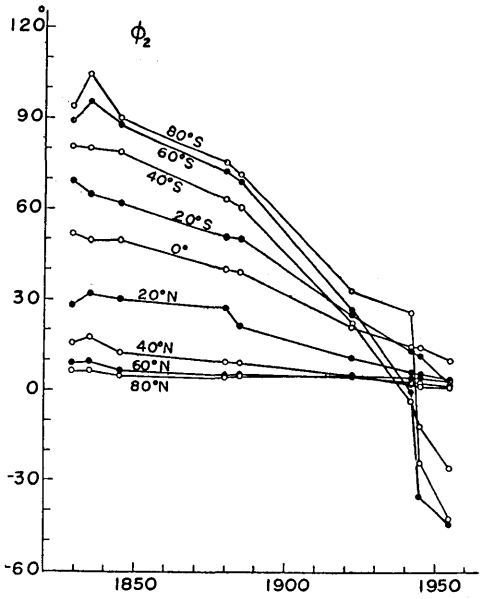

Fig. 2-1(c). ϕ_2

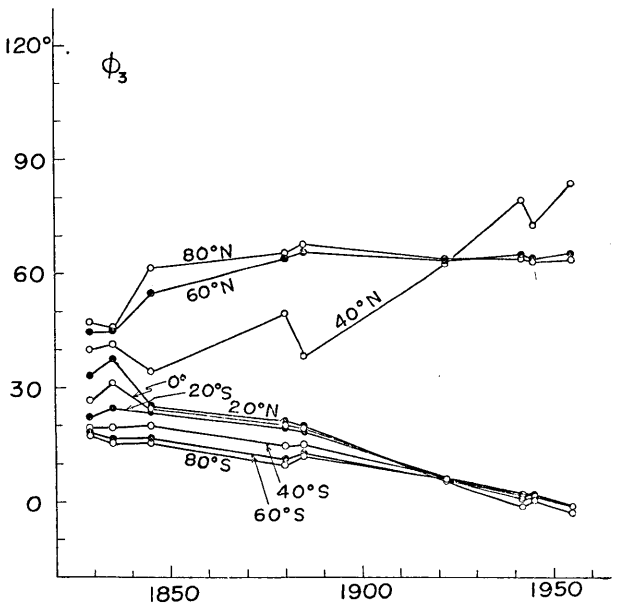

Fig. 2-1(d). ϕ_3

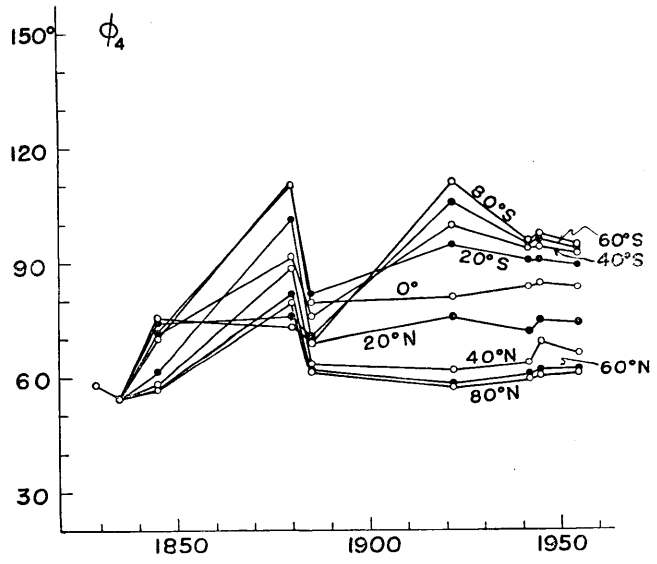

Fig. 2-1(e). ϕ_4

Fig. 2-1. Phase shift of magnetic potential at various latitudes

$$V=a\sum_m C_m \cos m(\lambda-\phi_m) \tag{2-3}$$

where

$$C_m=\sqrt{G_m^2+H_m^2}$$
$$\phi_m=\frac{1}{m}\tan^{-1}\frac{H_m}{G_m}\ .$$

The westward drift of the field will give rise to a monotonous decrease in ϕ_m as time passes on. ϕ_m's are calculated for latitude circles at intervals of twenty degrees from data[17] for various epochs since 1829. The results are shown in Table 2-1 and Fig. 2-1. A straight line is tentatively fitted to every set of 9 points. The slope of the lines is shown in Table 2-2 and Fig. 2-2.

Fig. 2-1a shows ϕ_1 for 9 latitude circles as a function of time. We can see a tendency for a westerly drift of ϕ_1 along every circle of latitude. Excepting the fairly quick motion along the 80°N circle, a velocity amounting to $0.062°/yr$ is obtained on an average. In order

17) E. H. VESTINE, L. LAPORTE, I. LANGE and W. I. SCOTT, *Carnegie Inst. Publ. No.* **580** (1947).

Table 2–1. Longitudes of harmonic components at 20° intervals of latitude

	Date	1829	1835	1845	1880	1885	1922	1942	1945	1955
ϕ_1	80°N	76.°0	70.°6	55.°2	53.°3	55.°2	51.°3	43.°2	37.°9	44.°6
	60	85.0	85.1	77.1	76.0	76.4	74.7	71.2	69.4	75.1
	40	96.6	97.8	95.9	93.5	97.7	92.8	94.2	93.3	96.6
	20	103.6	103.3	101.8	97.2	97.7	95.4	95.8	94.5	95.5
	0	109.4	109.7	108.5	103.5	104.3	100.9	99.5	98.5	98.7
	20	120.8	122.8	123.1	117.9	117.9	115.6	115.0	113.6	113.7
	40	137.8	141.5	139.4	125.3	131.9	133.0	134.2	132.2	132.2
	60	151.6	153.0	153.0	151.1	148.9	147.6	148.3	145.0	144.5
	80° S	156.7	157.2	161.4	158.2	160.0	155.8	155.3	150.3	149.8
	Date	1829	1835	1845	1880	1885	1922	1942	1945	1955
ϕ_1'	80°N	−15.°7	−27.°0	−16.°2	−21.°9	−23.°7	−30.°8	−36.°6	−39.°3	−41.°8
	60	−15.0	−21.5	−14.6	−23.2	−25.5	−36.1	−44.1	−45.4	−48.8
	40	−10.4	− 5.1	− 7.7	−22.2	−27.9	−38.1	−47.1	−48.7	−52.3
	20	3.3	16.6	1.7	−14.5	−14.0	−22.7	−26.9	−27.9	−32.0
	0	28.9	24.0	11.3	1.2	1.8	10.2	16.6	15.7	12.2
	20	167.3	192.2	167.2	149.5	148.3	136.2	128.7	129.0	124.4
	40	185.0	187.1	180.1	160.9	166.2	164.6	163.6	162.0	159·1
	60	188.1	183.3	189.0	177.8	182.1	176.0	174.6	169.9	167.7
	80° S	188.9	181.5	194.9	194.0	191.8	181.5	179.4	171.7	170.3
	Date	1829	1835	1845	1880	1885	1922	1942	1945	1955
ϕ_2	80°N	6.°6	6.°7	5.°0	4.°5	5.°0	5.°4	5.°0	5.°2	4.°2
	60	9.1	9.9	6.7	5.6	5.7	5.0	3.8	3.6	2.8
	40	15.6	17.8	12.7	9.9	9.4	5.9	3.2	2.5	2.0
	20	28.2	32.0	30.1	27.9	21.8	11.6	7.2	6.6	4.8
	0	51.8	49.5	49.8	40.3	39.4	21.6	15.6	15.4	11.2
	20	69.2	64.8	62.0	51.0	50.2	25.9	14.5	12.6	3.5
	40	80.6	80.0	78.6	63.5	60.9	23.0	− 2.4	−11.0	−24.5
	60	89.0	95.2	87.7	72.8	69.2	27.4	0.8	−34.4	−41.2
	80° S	93.7	104.2	89.9	75.6	71.5	33.8	26.9	−23.0	−43.3
	Date	1829	1835	1845	1880	1885	1922	1942	1945	1955
ϕ_3	80°N	47.°1	46.°0	61.°4	65.°4	67.°7	63.°7	63.°9	63.°0	63.°6
	60	44.8	44.8	55.0	64.0	65.6	63.6	64.9	63.6	65.1
	40	40.0	42.3	34.2	49.6	38.2	62.2	79.1	72.9	83.7
	20	33.1	37.8	25.2	21.0	19.9	5.2	− 1.6	0.0	− 3.3
	0	26.7	31.4	24.7	20.3	19.5	5.6	0.5	1.5	− 1.2
	20	22.2	24.7	23.6	19.2	18.2	6.1	1.3	1.9	− 1.0
	40	19.6	19.6	20.1	14.5	15.0	6.1	1.7	2.0	− 1.2
	60	18.1	16.7	16.9	11.1	12.9	5.7	1.7	1.8	− 1.3
	80° S	17.4	15.3	15.5	9.7	12.1	5.4	1.7	1.7	− 1.2

(To be continued)

	Date	1829	1835	1845	1880	1885	1922	1942	1945	1955
	80°N	57.8°	54.2°	56.7°	79.5°	61.3°	57.2°	59.5°	60.2°	60.7°
	60	57.8	54.2	57.0	81.9	61.8	58.3	60.0	61.8	61.9
	40	57.8	54.2	58.0	88.4	63.4	61.7	63.6	69.0	65.9
	20	57.8	54.2	61.2	101.2	68.6	75.5	71.4	74.7	73.9
ϕ_4	0	57.8	54.2	70.0	110.4	79.7	81.0	83.7	84.5	83.4
	20	57.8	54.2	71.1	110.2	81.8	94.8	90.4	90.5	89.1
	40	57.8	54.2	70.7	91.5	75.8	99.8	93.2	93.9	92.1
	60	57.8	54.2	74.0	75.7	70.5	105.8	94.6	96.0	93.8
	80° S	57.8	54.2	75.1	72.5	68.3	111.4	95.5	97.2	94.5

The authors of the data used in this calculation are listed below.

1829	Erman Petersen
1835	Gauss
1845	Adams
1880	Adams
1885	Fritsche
1922	Dyson Furner
1942	Jones Melotte
1945	Vestine and others
1955	Finch Leaton

to examine whether the equatorial dipole has a velocity different from that of the non-dipole field having the order m=1, the equatorial dipole term is excluded from the magnetic potential, and the variation in ϕ_1' which is defined by the following equations,

$$\left.\begin{aligned} G_1' &= \sum_{n=2} \left(\frac{a}{r}\right)^{n+1} g_n' P_n^1(\cos\theta) \\ H_1' &= \sum_{n=2} \left(\frac{a}{r}\right)^{n+1} h_n' P_n^1(\cos\theta) \end{aligned}\right\} \qquad (2\text{–}2)'$$

$$C_1' = \sqrt{G_1'^2 + H_1'^2}$$

$$\phi_1' = \tan^{-1}\frac{H_1'}{G_1'}$$

is studied. As can be seen in Fig. 2–1b, ϕ_1' drifts westwards with a velociy, $0.224°/yr$ on an average, which is larger than that of ϕ_1. We therefore see that the equatorial dipole, which has shown no marked rotation, greatly affects the drift velocity of ϕ_1 thus deter-

Table 2–2. Mean velocity of westward drift of harmonic components (unit in degree/year)

	$\dot{\phi}_1$	$\dot{\phi}_1'$	$\dot{\phi}_2$	$\dot{\phi}_3$
80°N	0.220	0.097	0.000	−0.012
60	0.073	0.275	0.050	−0.060
40	0.022	0.370	0.115	−0.384
20	0.070	0.318	0.216	0.295
0	0.085	0.075	0.339	0.250
20	0.070	0.391	0.580	0.230
40	0.057	0.168	0.970	0.188
60	0.053	0.146	1.11	0.165
80° S	0.067	0.180	1.10	0.148

mined. From these results, the geomagnetic field expressible by the equatorial dipole may be supposed to have an origin different from that of the non-dipole field having the order m=1. It seems likely that the equatorial dipole part of the geomagnetic field has something to do with the dynamo action predominating in the deep interior of the core, while the non-dipole field is believed to be caused by induction processes accompanying it. Fig. 2-1b shows that the velocities of ϕ_1'

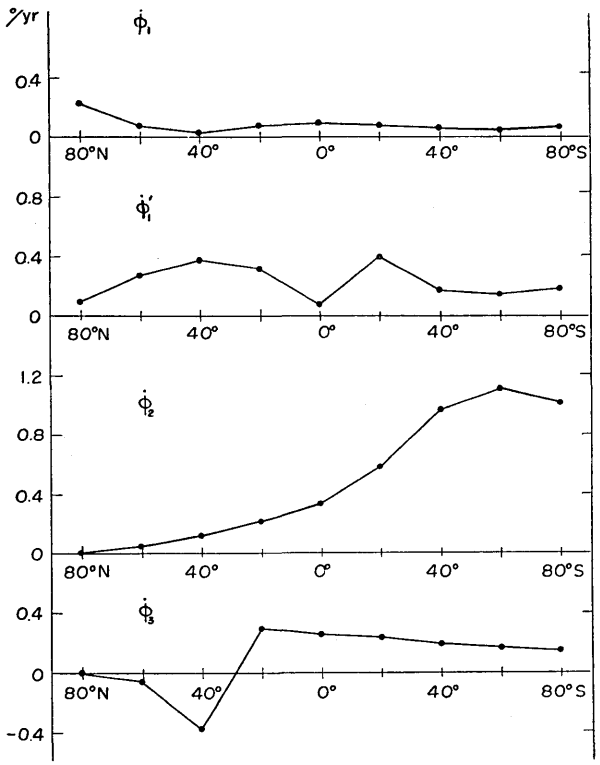

Fig. 2-2. Velocity of westward drift of harmonic components by the phase shift method. $\dot{\phi}_1'$ means the drift velocity for m=1 when the equatorial dipole is excluded.

obtained by this method are larger in the nothern hemisphere than in the southern hemisphere. An irregular drift is seen on the equator. Along the 20°S latitude the drift velocity is extraordinarily large. It is interesting to compare the phase shift of ϕ_1' with the distribution of the amplitude C_1' as is shown in Fig. 2-3. The intensity of C_1' becomes small on the equator and 20°S.

ϕ_2 decreases more rapidly with time accordingly as we proceed southwards (Fig. 2–1c), while it has hardly moved at 30°N and 60°N during the past 120 years. ϕ_3 shows rather an eastward drift at 80°N, 60°N and 40°N. Especially the eastward drift at 40°N is strong, the reason for which will be discussed later. ϕ_3 moves westwards, however, at 20°N, 0°, 20°S with a velocity of about $0.25°/yr$, and at 40°S, 60°S, 80°S with about $0.17°/yr$. As is shown in Fig. 2–1e, ϕ_4 varies rather irregularly with time. The cause of the irregularity is likely to be the inaccuracy of the spherical harmonic analyses for such a high order.

It may be noticed in Fig. 2–1c and d, that the earth's field can be divided into three zones by the parallels 30°N and 30°S and that ϕ_2 and ϕ_3 show the same type of time-variation according to the region to which they belong. There seem to be two possible explanations for the above characteristics. One is the consideration that the three zones, preserving every features unchanged, drift separately with respective velocity. The other is that some of the predominant features in every zone, which are expressible in terms of the harmonics $m=2$ and 3, move independently. By means of spherical harmonic analyses alone, it is not possible to determine which cause is the more likely.

The velocities of ϕ_2 in the southern hemisphere are extraordinarily large (Table 2–2, Fig. 2–1c, d), compared with those so far obtained by Bullard and others. The discrepancy can be removed by taking into account the distribution of the amplitude of each harmonic constituent on the earth's surface. The C_m in the equation (2–3) for various latitudes are calculated from Finch-Leaton's data[18] and are shown in Fig. 2–3. At the latitude of 40°N and 20°N the drift of ϕ_2 may be as reliable as the drift of ϕ_1', because the amplitude C_2 is nearly the same as C_1' at this latitude. The rapid decrease in the amplitude C_2 in the southern hemisphere suggests that the variation in ϕ_2 is less important than that of ϕ_3. On the other hand C_3 is small in the northern hemisphere and becomes large in the other. The smallness of C_3 at 40°N may cause the amplitude C_3 vary at a rapid rate, which seems to be the reason why ϕ_3 at the latitude appears to move eastwards faster than at any other latitude. The actually observed drift of the main features of the earth's field will be greatly affected by the harmonic component that has the largest amplitude at a specified latitude. Consequently Fig. 2–3 indicates that the westward drift of

18) H. F. FINCH and B. R. LEATON, *Mon. Not. Roy. Astro. Soc., Geophys. Suppl.*, **7** (1957), 314.

the geomagnetic field is mainly controlled by the drift of the non-dipole part of the harmonic component m=1, while the harmonics m=2 and

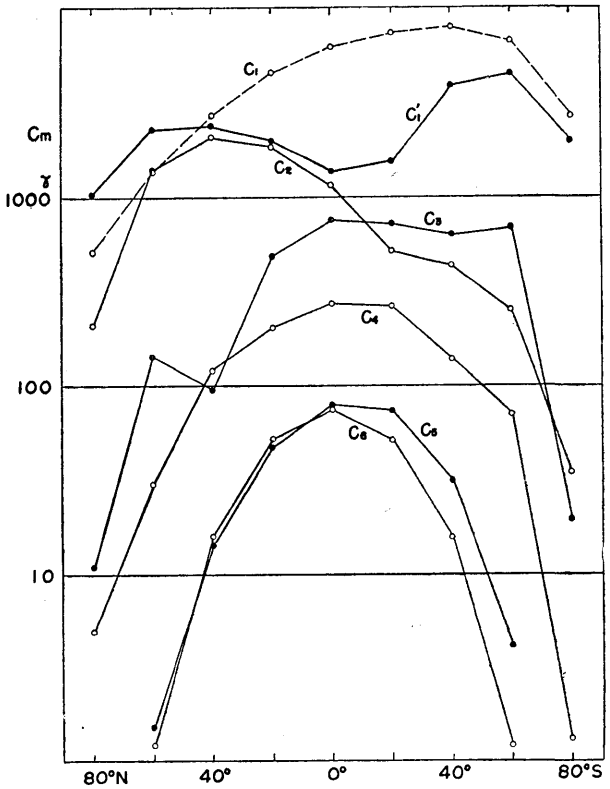

Fig. 2-3. Distribution of amplitudes of harmonics (calculated from Finch Leaton's data, 1955).

3 take part in the drift in the northern and the southern hemisphere respectively. This will be seen more clearly in the following section.

2-2. Drift velocity obtained from the analyses of the geomagnetic field and its rate of change.

We have a number of spherical harmonic analyses for the rate of change in the earth's magnetic field since 1902, which are often called "analyses of the secular variation" by reason that they are the analyses of change during ten year periods. Combining these with analyses of the earth's magnetic field itself, the drift velocity of the magnetic field

will be calculated in this section by means of the least square method with regard to space in a way similar to Whitham's analysis.

Let the scalar potential of the magnetic field and that of the rate of change at one epoch be V and $\partial V/\partial t$ respectively. We have

$$\left.\begin{aligned} V &= a\sum_{m=0}^{\infty}(G_m\cos m\lambda + H_m\sin m\lambda) \\ \frac{\partial V}{\partial t} &= a\sum_{m=0}^{\infty}(\dot{G}_m\cos m\lambda + \dot{H}_m\sin m\lambda) \end{aligned}\right\} \tag{2-4}$$

where G_m, H_m, $\dot{G}_m$ and $\dot{H}_m$ are written in terms of the Gaussian coefficients as follows,

$$\left.\begin{aligned} G_m &= \sum_{n=m}^{\infty}\left(\frac{a}{r}\right)^{n+1} g_n{}^m P_n{}^m(\cos\theta) \\ H_m &= \sum_{n=m}^{\infty}\left(\frac{a}{r}\right)^{n+1} h_n{}^m P_n{}^m(\cos\theta) \end{aligned}\right\} \tag{2-5}$$

$$\left.\begin{aligned} \dot{G}_m &= \sum_{n=m}^{\infty}\left(\frac{a}{r}\right)^{n+1} \dot{g}_n{}^m P_n{}^m(\cos\theta) \\ \dot{H}_m &= \sum_{n=m}^{\infty}\left(\frac{a}{r}\right)^{n+1} \dot{h}_n{}^m P_n{}^m(\cos\theta) \end{aligned}\right\} \tag{2-6}$$

In case all the components drift with a constant velocity v, we can calculate the residual field R in the equation (1–4) as follows

$$\begin{aligned} R &= \frac{\partial V}{\partial t} + v\frac{\partial V}{\partial \lambda} \\ &= a\sum_{m}\{(\dot{G}_m + vmH_m)\cos m\lambda + (\dot{H}_m - vmG_m)\sin m\lambda\} \end{aligned} \tag{2-7}$$

when each component moves with its own velocity v_m, the equation (2–7) is replaced by

$$R = a\sum_{m}\{(\dot{G}_m + v_m mH_m)\cos m\lambda + (\dot{H}_m - v_m mG_m)\sin m\lambda\} \tag{2-8}$$

After some calculation, Φ defined in the equation (1–5) becomes

$$\begin{aligned} \Phi &= a\int_0^{2\pi} R^2 d\lambda \\ &= \pi a^2 \sum_{m}[(\dot{G}_m + v_m mH_m)^2 + (\dot{H}_m - v_m mG_m)^2] \end{aligned} \tag{2-9}$$

The velocity that minimizes Φ is obtained as follows

$$v_m=-\frac{\dot{G}_m H_m-\dot{H}_m G_m}{m(G_m^2+H_m^2)}. \tag{2-10}$$

When the magnetic field drifts with a uniform velocity v, we have the following equations in place of the equations (2-9) and (2-10)

$$\Phi=\pi a^2 \sum_m [(\dot{G}_m+vmH_m)^2+(\dot{H}_m-vmG_m)^2] \tag{2-11}$$

$$v=-\frac{\sum_m m(\dot{G}_m H_m-\dot{H}_m G_m)}{\sum_m m^2(G_m^2+H_m^2)} \tag{2-12}$$

From these, the analyses of V and $\partial V/\partial t$ at the same epoch may serve to determine the distribution of the drift velocity for various latitudes.

The velocities at the epochs of 1922.5, 1942.5 and 1955.5 are calculated. The data used for the calculation are the combination of Dyson-Furner's analysis of V at 1922 and that of Vestine and others for $\partial V/\partial t$ at 1922.5, Jones-Melotte's V (1942) and Vestine and others' $\partial V/\partial t$ (1942.5) and for the computation of the velocity distribution at 1957.5 Finch-Leaton's data for V (1955) and Nagata-Syono's for $\partial V/\partial t$ (1957.5) are used. In order to see to what extent the results should be affected by making use of the V and $\partial V/\partial t$ of different dates, calculations for two different sets of data were carried out, one being a combination of analyses by Jones-Melotte (1942) for V and by Vestine and others (1942.5) for $\partial V/\partial t$ and the other being that of Vestine and others (1945) for V and Vestine and others (1942.5) for $\partial V/\partial t$. The test clarified that the differences in the velocities obtained from the two sets of data were negligibly small. Consequently it should be permissible to use Finch-Leaton's data for 1955 in place of data for 1957.5 for the computation of the velocity at that epoch.

The results of the calculation are shown in Table 2-3 and Fig. 2-4. Fig. 2-4 shows the velocity distributions of the westward drift corresponding to each harmonic component. The magnetic field represented by m=1 moves westwards with a very small velocity of about 0.1°/*yr*, except in the regions of high latitude in the northern hemisphere. The magnetic field of m=2 hardly moves at the high latitudes in the northern hemisphere. Its drift velocity increases gradually towards the south exceeding 1°/*yr* in the southern hemisphere. At 80°N and 60°N

the field of m=3 appears to move eastwards with velocities of about 0.1°/*yr* and 0.16°/*yr*. Especially at 40°N a marked eastward drift is observed. These features agree very well with the results of the phase

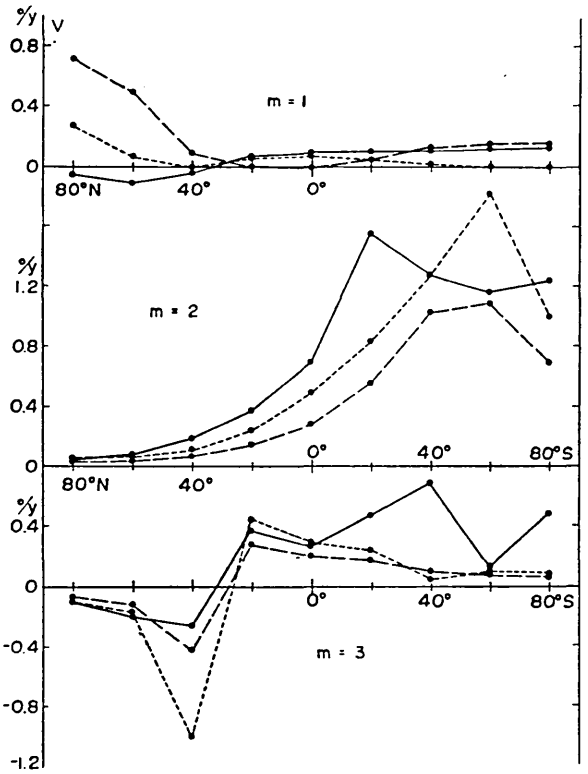

Fig. 2-4. Velocity of westward drift for harmonic components at different epochs. Solid lines, 1957.5: broken lines 1942.5: dotted lines, 1922.5.

shift method which are shown in Fig. 2–2 or Table 2–2. In view of the present knowledge such a large velocity as in the case of m=2 in the southern hemisphere is unacceptable. No westerly drift faster than 0.5°/*yr* has been reported as yet. In Bullard's study (1950) we can see a similar situation. Comparing two charts of the rate of change $\partial V/\partial t$ at 30 year intervals, Bullard and others calculated the velocity distributions for various latitudes as in Fig. 2–5 and obtained a mean velocity 0.32°/*yr*, which is different from the velocity 0.18°/*yr* obtained by applying the same method to the charts of the non-dipole field

Table 2-3. Drift velocity of harmonic components at three different epochs (unit in °/*yr*)

(A) Vestine et al (1920-1925)—Dyson Furner (1922)

	m=1	m*=1	m=2	m=3	Mean
80°N	0.256	0.396	0.047	−0.105	0.345
60	0.056	0.426	0.062	−0.172	0.187
40	−0.010	0.373	0.107	−1.027	0.154
20	0.055	0.149	0.240	0.440	0.236
0	0.067	−0.117	0.487	0.291	0.353
20	0.038	0.302	0.833	0.238	0.402
40	0.014	0.130	1.265	0.043	0.145
60	−0.001	0.084	1.815	0.092	0.092
80° S	−0.005	0.074	0.994	0.071	0.075

(B) Vestine et al (1940-1945)—Jones Melotte (1942)

	m=1	m*=1	m=2	m=3	Mean
80°N	0.710	0.202	0.025	−0.078	0.176
60	0.481	0.196	0.033	−0.131	0.093
40	0.081	0.249	0.062	−0.432	0.099
20	−0.010	0.334	0.140	0.271	0.188
0	−0.019	−0.300	0.274	0.194	0.196
20	0.044	0.230	0.556	0.162	0.240
40	0.122	0.269	1.209	0.097	0.242
60	0.154	0.209	1.835	0.069	0.205
80°S	0.158	0.181	0.686	0.057	0.181

(C) Nagata Syono (1955-1960)—Finch Leaton (1955)

	m=1	m*=1	m=2	m=3	Mean
80°N	−0.062	0.109	0.040	−0.117	0.115
60	−0.120	0.143	0.074	−0.202	0.200
40	−0.051	0.211	0.178	−0.262	0.266
20	0.064	0.339	0.368	0.374	0.275
0	0.089	0.415	0.686	0.260	0.208
20	0.096	0.486	1.551	0.471	0.272
40	0.110	0.284	1.276	0.685	0.226
60	0.116	0.225	0.611	0.128	0.228
80°S	0.124	0.246	0.558	0.441	0.246

The columms of m*=1 represent the drift velocity of the non-dipole part of m=1 after excluding the equatorial dipole.

V. It is noticeable that the curve in the northern hemisphere in Fig. 2-5 resembles those of ours for m=2 in Fig. 2-4.

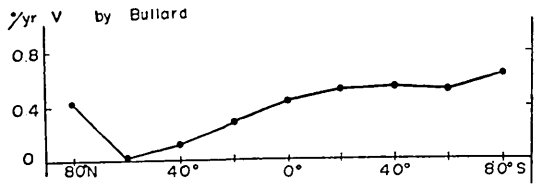

Fig. 2-5. Westward drift velocity of rates of change in the field obtained by Bullard and others.

Bullard computed the difference ε in the rate of change in the field $\dot{H}$, in the two maps

$$\varepsilon=\dot{H}_{1942.5}(\phi)-\dot{H}_{1912.5}(\phi+D)$$

and determined D by making the summation $\sum\varepsilon^2$ minimum. The above equation can be written in the same form as the equation (1-7)

$$\varepsilon\approx[\dot{H}_{1942.5}(\phi)-\dot{H}_{1912.5}(\phi)]-D\dot{D}\frac{\partial^2 H_{1912.5}(\phi)}{\partial\phi^2}.$$

This is an equation involving the second order derivative, so that more weight is put on the higher harmonics than in the equation (1-7) in the case of the non-dipole field.

As is already stated, the trouble can be solved by taking into account the amplitude of each component. As the non-dipole parts for the harmonic m=1 should be discriminated from the equatorial dipole, the drift velocity of the non-dipole parts for m=1 are calculated, replacing G_1, H_1, $\dot{G}_1$ and $\dot{H}_1$ in the equations (2-5), (2-6) by the G_1', H_1', $\dot{G}_1'$ and $\dot{H}_1'$.

$$\left.\begin{aligned} G_1'&=\sum_{n=2}\left(\frac{a}{r}\right)^{n+1} g_n' P_n^1(\cos\theta)\\ H_1'&=\sum_{n=2}\left(\frac{a}{r}\right)^{n+1} h_n' P_n^1(\cos\theta)\end{aligned}\right\} \qquad (2\text{-}13)$$

$$\left.\begin{aligned} \dot{G}_1'&=\sum_{n=2}\left(\frac{a}{r}\right)^{n+1} \dot{g}_n' P_n^1(\cos\theta)\\ \dot{H}_1'&=\sum_{n=2}\left(\frac{a}{r}\right)^{n+1} \dot{h}_n' P_n'(\cos\theta)\end{aligned}\right\} \qquad (2\text{-}14)$$

As is shown in the upper diagram of Fig. 2–6, the velocity seems nearly constant except at the equator. The results also indicate that the non-dipole part having m=1, differs essentially from the equatorial dipole when compared with those shown in the top diagram in Fig. 2–4. In the southern hemisphere, the large velocity derived from

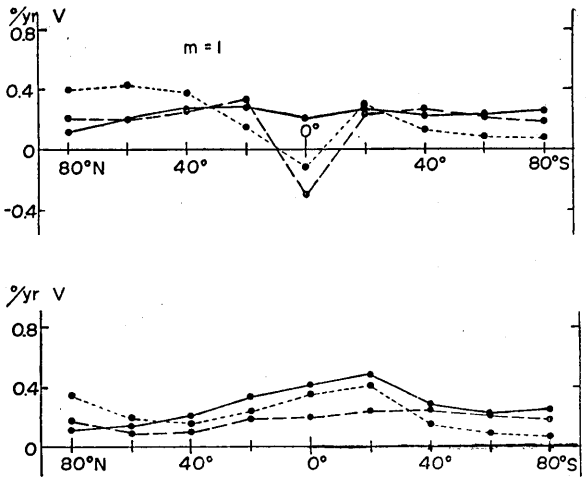

Fig. 2-6. Velocity of westward drift of magnetic potentials at different epochs. (Solid lines, 1957.5: broken lines, 1942.5: dotted lines, 1922.5).
The top diagram represents the velocities of the non-dipole part of m=1; i.e. the velocities when the equatorial dipole is excluded. The bottom diagram represents the velocities when all harmonics move with the same velocity.

harmonic m=2 seems to take no significant part, because of the overwhelming intensity of C_1 (Fig. 2–3). In the northern hemisphere the predominance of C_1 and C_2 seems to conceal the eastward drift of the harmonic component m=3. These troublesome phenomena are likely to be caused partly by the seperate treatment of each harmonic. The velocity v when the non-dipole field uniformly rotates is calculated by the equation (2–12), substituting G_1', H_1', $\dot{G}_1'$ and $\dot{H}_1'$ in place of G_1, H_1, $\dot{G}_1$ and $\dot{H}_1$. The results are shown in the lower diagram of Fig. 2–6. At 20°S the maximum velocity appears. Although the obtained velocities fluctuate from $0.1°/yr$ to $0.4°/yr$, the mean velocity of about $0.2°/yr$ is consistent with those obtained by other authors.

2-3. Concluding remarks.

Good agreement can be seen between the results obtained by the two different methods, the method of the phase shift and that of the least square for the residual field. They are summarized as follows.

a) The magnetic field represented by m=1 can be divided into two parts that move with different velocities, *i.e.*, the field of the equatorial dipole having a velocity of about $0.1°/yr$, and that of the non-dipole expressed in terms of $P_2^1(\theta)$, $P_3^1(\theta)$ etc. with a velocity of about $0.2°/yr$. This suggests that the equatorial dipole and the non-dipole parts of m=1 are produced by a different mechanism.

b) The drift velocity for harmonic components m=2 and m=3 do not show such a simple distribution as that for m=1, of which the velocity is approximately independent of the latitude. The obtained velocity for m=2 increases rapidly in the southern hemisphere. The magnetic field for m=3 at high latitudes in the northern hemisphere seems to move rather eastwards.

The fact that the velocity of the field obtained for m=1 is fairly uniform throughout every latitude and that the different methods for different epochs give well-agreeing results suggests strongly that the observed rate of change in the field is mostly caused by the westward drift. The peculiar behaviour of the magnetic field represented by m=2 and m=3 as is stated in (b), is closely related to the amplitude distribution of the corresponding term of the field. It is clear that the intensity much weaker than the predominant term m=1 is the cause of the phenomena. Accordingly as the amplitude becomes smaller, the field will be readily changed at a rapid rate even by a small fluctuation of the fluid motion. Details of this phenomena of small scale are left for future work.

Chaper 3. The Westward Drift and the Observed Time Variation in the Magnetic Field.

3-1. Introduction.

There are two causes responsible for the observed time variation in the earth's field, as we have seen in the preceding chapters; the westward drift of the magnetic field and the hydromagnetic process

taking place in the fluidal core. In view of the study of the previous chapter, it has become clear that the non-dipole field occupies the main part of the westward drift of the earth's magnetic field while the drift of the equatorial dipole field is very small. In order to bring out the nature of the westward drift more clearly, some further study on the drift is undertaken in this chapter from a stand point which is different from that in the former chapters. Magnetic data from 34 stations at which observations have been continued over fifty years are analysed in this chapter. After calculating the drift velocity by means of the integration with regard to time (A-method in (1–5)), we try to seperate the variation caused by the westward drift from the residual field.

3–2. Distribution of magnetic observatories.

Most of magnetic data used are collected from the publications by Fleming-Scott[19),20),21)] (1943, 1944, 1948) and Johnston[22),23)] (1951, 1956). As for recent observations, Professor Nagata has kindly given the writer

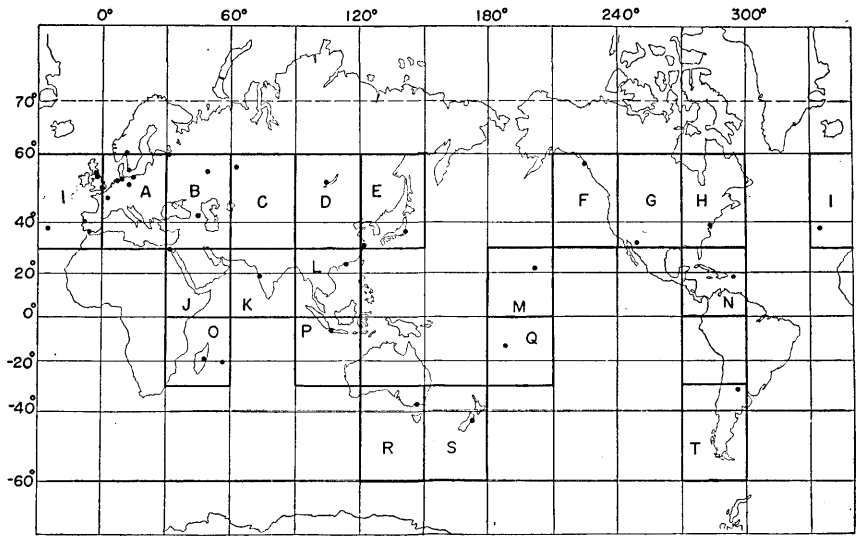

Fig. 3-1. Distribution of observatories

19) J. A. FLEMING and W. E. SCOTT, *Terr. Mag.*, **48** (1943), 97, 171, 237.
20) J. A. FLEMING and W. E. SCOTT, *Terr. Mag.*, **49** (1944), 47, 109, 199, 267.
21) J. A. FLEMING and W. E. SCOTT, *Terr. Mag.*, **53** (1948), 199.
22) H. F. JOHNSTON, *Jour. Geophys. Res.*, **56** (1951). 431.
23) H. F. JOHNSTON, *Jour. Geophys. Res.*, **61** (1956), 273.

Table 3-1. The localities of the observatories and the periods of observation

	Observatory	Lat.	Long.	Period
1	Slutsk	59°41′N	30°29′E	1869–1959
2	Oslo	59:55	10:43	1820–1948
3	Sitka	57:03	220:40	1902–1959
4	Sverdlovsk	56:44	61:04	1887–1959
5	Rude Skov	55:51	12:27	1892–1959
6	Zaimitche-Kasan	55:50	48:51	1894–1958
7	Eskdalemuir	55:19	356:48	1908–1959
8	Stonyhurst	53:51	357:32	1865–1943
9	Wingst	53:45	9:04	1884–1959
10	Witteveen	52:49	6:40	1891–1959
11	Irkutsk	52:17	104:16	1887–1958
12	Niemegk	52:04	12:40	1908–1959
13	Greenwich	51:11	359:37	1841–1959
14	Chambon-la-Forét	48:01	2:16	1883–1954
15	Dusheti	42:05	44:42	1879–1959
16	Coimbra	40:12	351:35	1866–1959
17	Cheltenham	38:44	283:10	1901–1956
18	San Miguel	37:46	334:21	1911–1959
19	San Fernando	36:28	353:48	1891–1959
20	Kakioka	36:14	140:11	1897–1959
21	Tucson	32:15	249:10	1901–1959
22	Zo-sê	31:06	121:11	1875–1947
23	Helwan	29:52	31:20	1903–1957
24	Au Tau	22:27	114:03	1884–1939
25	Honolulu	21:19	201:56	1902–1959
26	Alibag	18:38	72:52	1848–1958
27	San Juan	18:23	293:53	1903–1959
28	Batavia	− 6:11	106:49	1884–1945
29	Samoa Apia	−13:48	188:14	1905–1959
30	Tananarive	−18:55	47:32	1890–1958
31	Mauritius	−20:06	57:33	1897–1959
32	Pilar	−31:40	296:07	1905–1956
33	Toolangi	−37:32	145:28	1893–1956
34	Amberley	−43:10	172:44	1902–1959

permission to use his unpublished collection of data.

Some of the stations have been compelled to move to new sites as the disturbance field of artificial origin increases. In such cases, the discontinuous changes that accompanied the transfer of a station are corrected either by the published correction constants or by those inferred from the rate of change. Records of old sites were, in principle, reduced to those at new sites except in a few observatories. 34 stations having records for more than fifty years were selected and listed in Table 3-1 together with their localities and the periods of observation used in this analysis. The distribution of the observatories is also shown in Fig. 3-1.

3-3. Calculation of the apparent drift velocity.

We first assume that the residual field R in equation (1-4) is so small and random that it can be ignored when integrated over a sufficient interval of time. In the actual calculation, the following summation is taken instead of integration during the period of observation at every station.

$$\begin{aligned} \Phi &= \sum R^2 \\ &= \sum \left[\frac{\partial H}{\partial t} + (v_0 \cdot \nabla) H \right] \end{aligned} \tag{3-1}$$

where $\partial H/\partial t$ is the rate of change in the field at one station and H of the second term is the distribution of the magnetic field along the circle of latitude passing through the observatory. The most probable rate of drift v_0 are determined so as to make the summation Φ a minimum for the three components of the field at every observatory. If the probable velocity thus obtained at every station shows no serious contradiction one with another, it may be possible to justify the assumption that the residual field is small.

As the usual method of numerical differentiation based on the interpolation method necessarily amplifies the observational errors involved in the original data, observational results for a certain interval of time are approximated with a parabolic curve and its gradient at the centre of the interval is regarded as the time derivative of the field at that time. This is a sort of averaging process by which influences of a few exceedingly scattered values can be avoided, unlike the case of the interpolation method. Let (X, Y, Z) be the northerly,

easterly and vertical (positive downwards) components of the magnetic field H respectively. We may approximate the field variation for a period of $(2s+1)$ years by the following equation.

$$X_k(t_i)=A_k(t_i-t_k)^2+B_k(t_i-t_k)+C_k \quad \text{for} \quad [t_{k-s},\ t_{k+s}] \tag{3-2}$$

where t_i and t_k are the yearly time in units. Applying the least square method to the difference between the observed $X(t_i)$ and the $X_k(t_i)$ defined in the above within the region $[t_{k-s},\ t_{k+s}]$, A_k, B_k and C_k are determined as follows

$$A_k=\frac{(2s+1)\sum_{i=k-s}^{k+s}X(t_i)(t_i-t_k)^2-\sum_{i=k-s}^{k+s}X(t_i)\sum_{i=k-s}^{k+s}(t_i-t_k)^2}{(2s+1)\sum_{i=k-s}^{k+s}(t_i-t_k)^4-\sum_{i=k-s}^{k+s}(t_i-t_k)^2\sum_{i=k-s}^{k+s}(t_i-t_k)^2}$$

$$B_k=\frac{\sum_{i=k-s}^{k+s}X(t_i)(t_i-t_k)}{\sum_{i=k-s}^{k+s}(t_i-t_k)^2}$$

$$C_k=-\frac{\sum_{i=k-s}^{k+s}X(t_i)(t_i-t_k)^2\sum_{i=k-s}^{k+s}(t_i-t_k)^2-\sum_{i=k-s}^{k+s}X(t_i)\sum_{i=k-s}^{k+s}(t_i-t_k)^4}{(2s+1)\sum_{i=k-s}^{k+s}(t_i-t_k)^4-\sum_{i=k-s}^{k+s}(t_i-t_k)^2\sum_{i=k-s}^{k+s}(t_i-t_k)^2}\ .$$

Differentiating the equation (3-2) with respect to time, we have an approximate rate of change $\dot{X}_k(t_i)$ during the interval $[t_{k-s},\ t_{k+s}]$ as follows

$$\dot{X}_k(t_i)=2A_k(t_i-t_k)+B_k\ .$$

The value $\dot{X}_k(t_k)$ at the centre of the interval concerned is adopted as the best approximation for the rate of change $\dot{X}(t_k)$, that is to say,

$$\dot{X}(t_k)=B_k=\frac{\sum_{i=k-s}^{k+s}X(t_i)(t_i-t_k)}{\sum_{i=k-s}^{k+s}(t_i-t_s)^2}\ . \tag{3-3}$$

The same process is repeated with regard to the interval $[t_{k-s+1},\ t_{k+s+1}]$,

and the values of $\dot{X}(t_{k+1})$ are obtained. The most probable rate of change $\dot{X}(t)$ can thus be calculated over all the range of time.

In our case, six year intervals are taken as the piecewise interval, that is, $s=3$ is adopted. The equation (3–3) can be simply rewritten in the following form,

$$\dot{X}(t_k)=\frac{1}{28}[\{X(t_{k+1})-X(t_{k-1})\}+2\{X(t_{k+2})-X(t_{k-2})\}+3\{X(t_{k+3})-X(t_{k-3})\}]$$

The rate of change every year is calculated by this equation.

The distributions of the non-dipole field at 1945 which were computed by Bullard and others from Vestine's data are adopted as the spatial distribution of the magnetic field in the equation (3–1). Distributions of the non-dipole field along the circle of latitude passing through the observatory are constructed for each component of the field. For the purpose of numerical calculation the field values are read off from the distribution curves at 5° intervals and the fields between the read values are interpolated by the Stirling's formula.

Let the magnetic field read from the distributions at the interval of $\Delta\lambda$ be $X(\lambda_k)$. Then the magnetic field in the region

$$\left[\lambda_k-\frac{\Delta\lambda}{2},\ \lambda_k+\frac{\Delta\lambda}{2}\right]$$

can be approximated by the following equation,

$$X(\lambda)=X(\lambda_k)+\Delta X(\lambda_k)\cdot u+\Delta^2X(\lambda_k)\frac{u^2}{2} \qquad (3\text{–}4)$$

where

$$\Delta X(\lambda_k)=\frac{X(\lambda_{k+1})-X(\lambda_{k-1})}{2}$$

$$\Delta^2X(\lambda_k)=X(\lambda_{k+1})-2X(\lambda_k)+X(\lambda_{k-1})$$

$$u=\frac{1}{\Delta\lambda}(\lambda-\lambda_k)\ .$$

Being defined piecewise within each region of $\Delta\lambda$, $X(\lambda)$ is not always continuous at

$$\lambda=\lambda_k-\frac{\Delta\lambda}{2} \quad \text{or} \quad \lambda_k+\frac{\Delta\lambda}{2}\ .$$

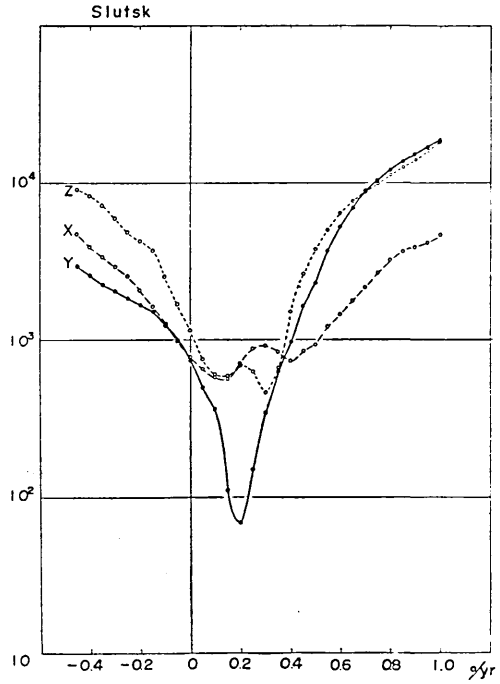

Fig. 3-2(a). Variation of $\emptyset$ with velocity at Slutsk.

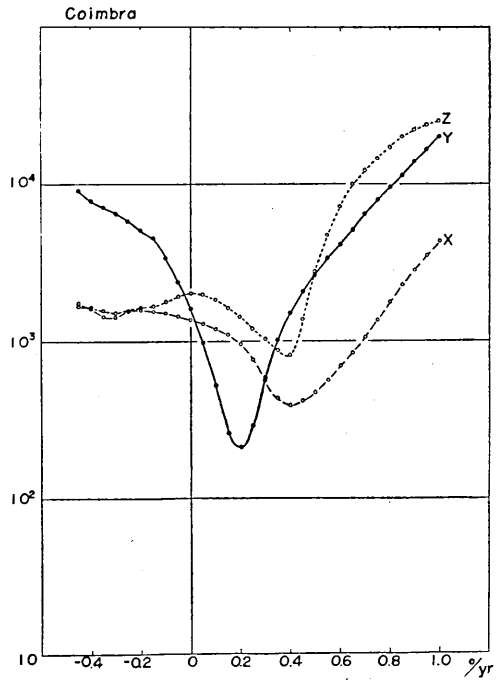

Fig. 3-2(b). Variation of $\emptyset$ with velocity at Coimbra.

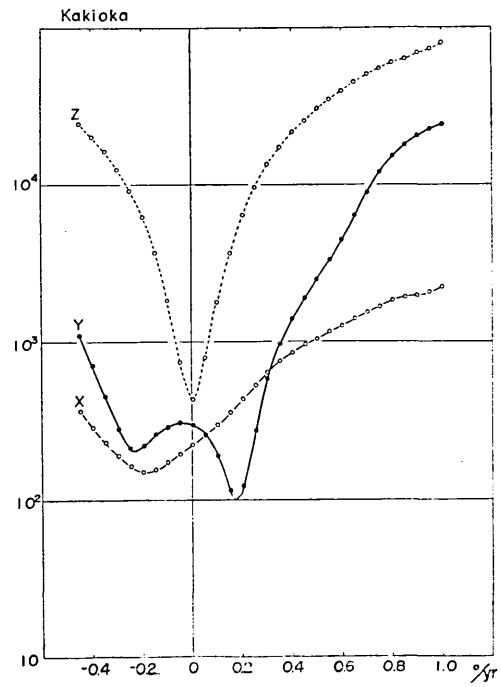

Fig. 3-2(c). Variation of $\emptyset$ with velocity at Kakioka.

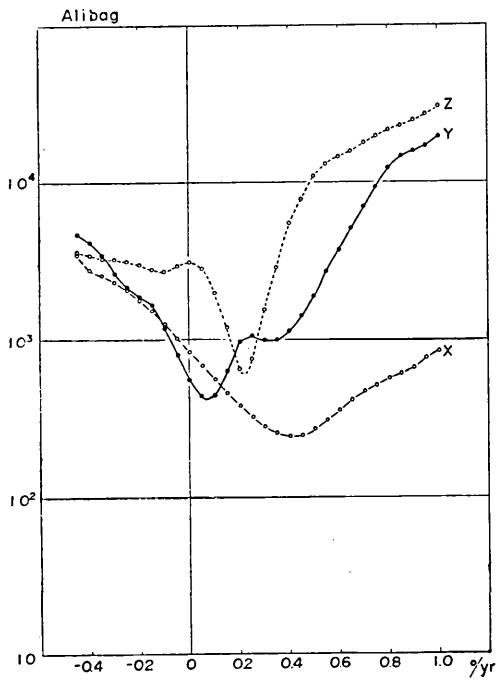

Fig. 3-2(d). Variation of $\emptyset$ with velocity at Alibag.

The discontinuity sometimes amounts to 100γ. The discontinuous change of this magnitude may well be ignored in most cases, however, because the variations in the magnetic field along a certain latitude circle are much larger.

When the magnetic field at an epoch t_0 is drifting with a westward velocity v, the change in the field caused by the drift at longitude ϕ_0 can be estimated as follows,

$$v\frac{\partial X}{\partial \lambda}=\frac{v}{\Delta\lambda}[\Delta X(\lambda_k)+\Delta^2 X(\lambda_k)\cdot u] \tag{3-5}$$

where λ satisfies the equation $\lambda=v(t-t_0)+\phi_0$.

Substituting these and the results of the computation of the equation (3-3) into the following Φ,

$$\Phi=\sum_k\left[\dot{X}(t_k)-v\frac{\partial X(t_k)}{\partial \lambda}\right]^2 \tag{3-6}$$

we can assess the most probable velocity by making Φ a minimum. The function Φ for each component at every station is calculated for the velocities between $-0.45°/yr$ and $1.00°/yr$ at an interval $0.05°/yr$. After the velocity which minimizes Φ is obtained, the same procedure was carried out at an interval $0.01°/yr$ around the velocity value obtained by the first approximation. A few examples are shown in Fig. 3-2. There often appear two minima in Φ as in Fig. 3-2a. In these cases, the velocity which is supposed to have more significance from the physical point of view was adopted.

3-4. The velocity of the westward drift.

The above stated method of determining the drift velocity was conducted for the three components of the magnetic field at 34 stations all over the world. The results are shown in Table 3-2 together with the probable errors in the velocity. With regard to a few observatories, the expected variations in the rate of change and the field intensity itself, by the westward drift of the non-dipole field with the velocities determined, are shown by solid curves in Figs. 3-3 and 3-4. At almost all the stations except those in the Pacific region good similarities are seen between the observed and the calculated variations.

The uncertainties of the velocity listed in Table 3-2 are estimated on the assumption that the differences between the observed and the

Table 3-2. Velocities of westward drift for the geomagnetic components at each station (°/*yr*)

	Observatory	V (X)	V (Y)	V (Z)
1	Slutsk	0.40±0.010	0.19±0.008	0.31±0.029
2	Oslo	0.42±0.012	0.17±0.011	0.43±0.004
3	Sitka	−0.07±0.003	−0.34±0.006	−0.22±0.011
4	Sverdlovsk	0.30±0.021	−0.26	0.08±0.004
5	Rude Skov	0.09±0.004	0.23±0.003	0.58
6	Zaimitche Kasan	0.36±0.005	0.10±0.001	0.14±0.001
7	Eskdalemuir	0.44	0.22±0.002	0.35
8	Stonyhurst	0.42±0.006	0.18±0.007	0.42
9	Wingst	0.43	0.22±0.011	0.78
10	Witteveen	0.44	0.23±0.007	0.48
11	Irkutsk	0.40±0.011	0.07±0.003	0.23±0.002
12	Niemegk	0.06±0.001	0.28±0.005	0.12±0.002
13	Greenwich	0.44±0.011	0.18±0.003	0.27±0.006
14	Chambon-la-Forét	0.51±0.008	0.22±0.009	0.45±0.008
15	Dusheti	0.40±0.011	0.35±0.009	0.16±0.004
16	Coimbra	0.41±0.051	0.19±0.006	0.39±0.011
17	Cheltenham	0.49±0.080	0.06±0.002	0.16±0.003
18	San Miguel	0.32±0.006	0.15±0.001	0.43±0.007
19	San Fernando	0.42±0.004	0.19±0.004	0.46
20	Kakioka	−0.18±0.005	0.17±0.003	0.00
21	Tucson	0.09±0.003	0.24±0.001	−0.30±0.004
22	Zo-sê	−0.23±0.002	0.07±0.002	−0.03±0.001
23	Helwan	0.35±0.009	0.41±0.005	0.16±0.004
24	Au Tau	−0.20±0.003	0.14±0.004	−0.06±0.001
25	Honolulu	−0.30±0.013	0.02±0.001	0.00
26	Alibag	0.41±0.033	0.32±0.020	0.22±0.001
27	San Juan	0.27±0.006	0.23±0.002	0.41±0.048
28	Batavia	0.05	0.54	0.59
29	Samoa Apia	0.26±0.008	0.30	0.07
30	Tananarive	−0.24±0.001	0.41±0.009	0.48±0.006
31	Mauritius	−0.14±0.003	0.43±0.036	0.62±0.008
32	Pilar	0.62±0.008	0.23±0.009	0.09±0.001
33	Toolangi	0.03	0.13±0.008	−0.22±0.004
34	Amberley	−0.17±0.002	0.26±0.007	−0.01±0.000

calculated rate of change in the field are caused by accidental errors in the velocity. If the deviation (δv) from the most probable velocity (v_0) is small, the difference $\delta\dot{X}(t_k)$ between the observed and the calculated rate of change can be written as follows,

$$\delta\dot{X}(t_k)=\frac{\partial\dot{X}(t_k)}{\partial v}\delta v$$

$$=(t_k-t_0)\frac{\partial\dot{X}(t_k)}{\partial\lambda}\delta v$$

By making use of the identity

$$\frac{\partial\dot{X}(t_k)}{\partial t}=v_0\frac{\partial\dot{X}(t_k)}{\partial\lambda}\ ,$$

we have,

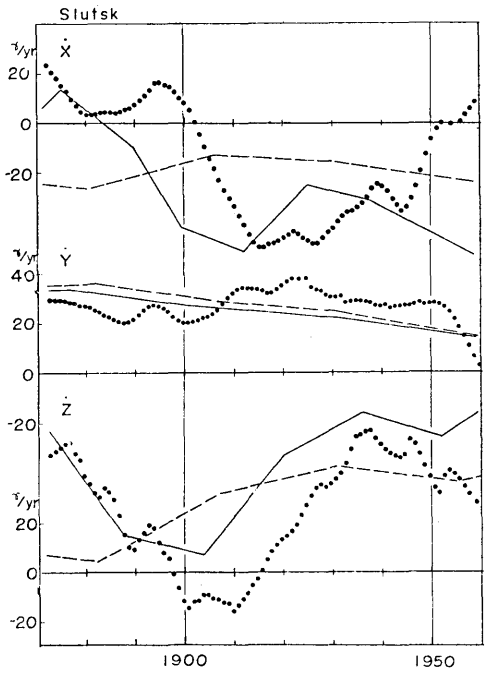

Fig. 3-3(a). Slutsk

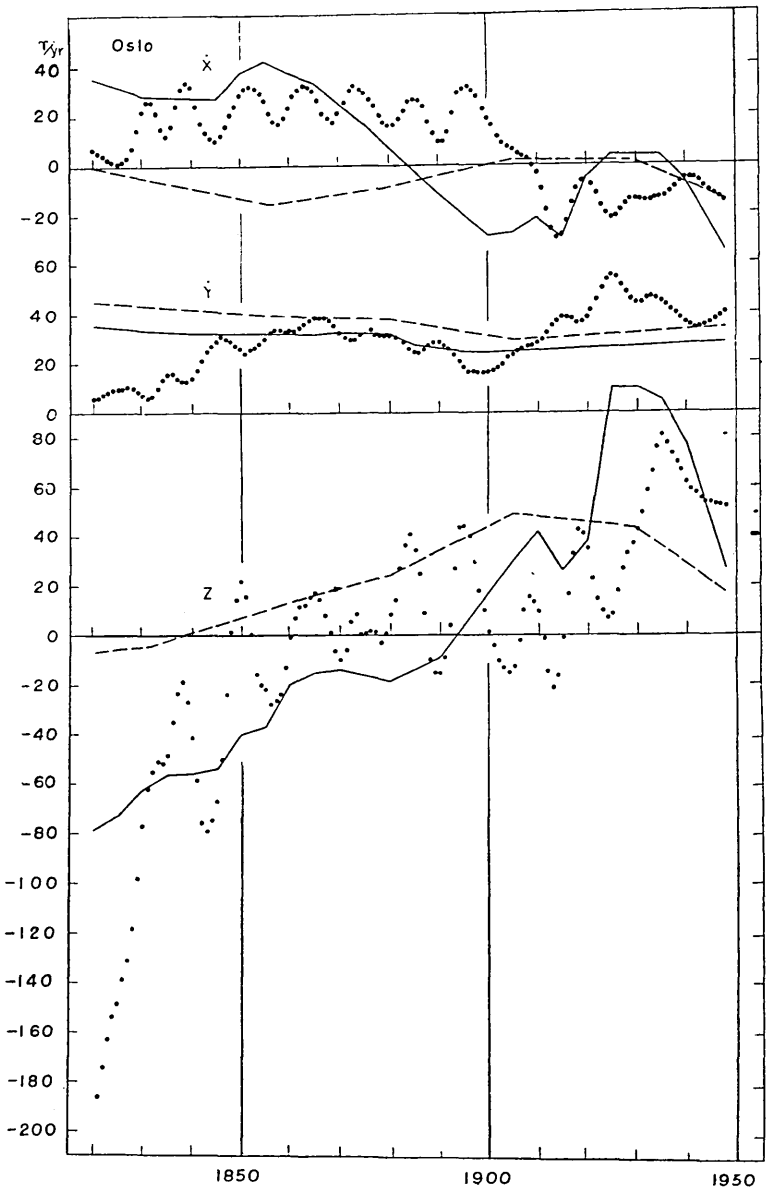
γ/yr
Oslo
Ẋ
Ẏ
Z
40
20
0
-20
60
40
20
0
80
60
40
20
0
-20
-40
-60
-80
-100
-120
-140
-160
-180
-200
1850
1900
1950

Fig. 3-3(b). Oslo

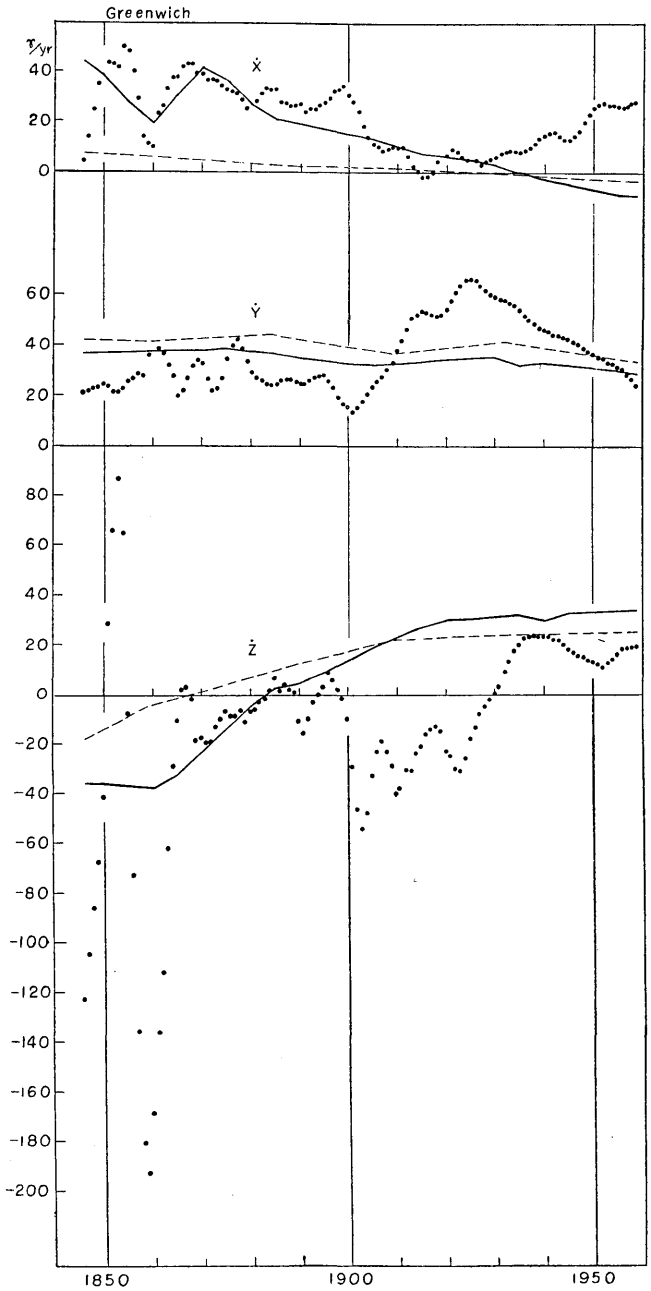

Fig. 3-3(c). Greenwich

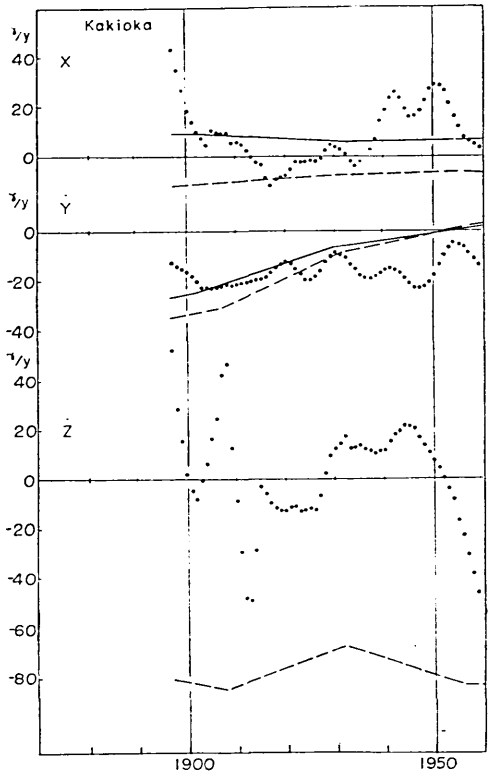

Fig. 3-3(d). Kakioka

$$\delta v = \frac{v_0}{\dfrac{\partial \dot{X}(t_k)}{\partial t}} \cdot \frac{\delta \dot{X}(t_k)}{t_k - t_0} .$$

Therefore the standard deviation $\sigma(\delta v)$ is obtained as follows,

$$\sigma^2(\delta v) = \frac{v_0^2}{T} \sum_{k=1}^{T} \left[\frac{1}{\dfrac{\partial \dot{X}(t_k)}{\partial t}} \cdot \frac{\partial \dot{X}(t_k)}{t_k - t_0} \right]^2 \qquad (3\text{-}7)$$

where T is the period of observation.

Simple averages of the velocity thus obtained over the northern and southern hemisphere, or all over the world, are listed in Table 3-3.

Fig. 3-5 shows how the velocities thus obtained are distributed at various latitudes. No marked dependency on latitude can be seen for

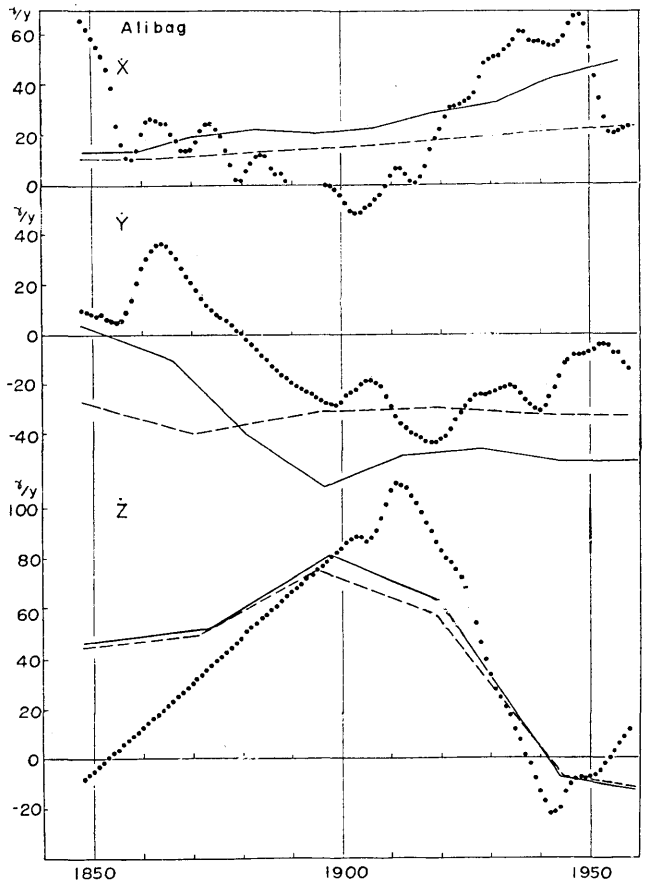

Fig. 3-3(e). Alibag

Fig. 3-3. Rate of change in the field at various stations. Solid lines show the rate of variation when field drifts with the local velocity which is determined by the least square method. Broken lines represent the variation due to the westward drift with uniform velocity, 0.20°/yr.

Table 3-3. Simple means of the velocities over the northern and the southern hemisphere (unit in °/*yr*)

	Northern hemisphere	Southern hemisphere	Throughout the world
V (X)	0.255±0.018	0.059±0.005	0.215±0.016
V (Y)	0.157±0.006	0.329±0.004	0.192±0.006
V (Z)	0.238±0.014	0.231±0.005	0.236±0.013

each component. The values for the north and the vertical component are much scattered, while those for the east component show a fairly good agreement with one another. The velocity for the east component seems slightly faster in the southern hemisphere than in the other. The variation curves of the drift velocity in Fig. 2–6, which were computed from the magnetic potentials, are depicted on the diagram for the east component (Fig. 3–6). The velocity distributions obtained independently show a good agreement with each other.

In order to examine further the property of the scattering in the north and the vertical component, the velocities are plotted in Fig. 3–7 against longitude. The decrease in the velocity in the Pacific region and the large velocities something like $0.4°/yr$ in Europe are noticeable

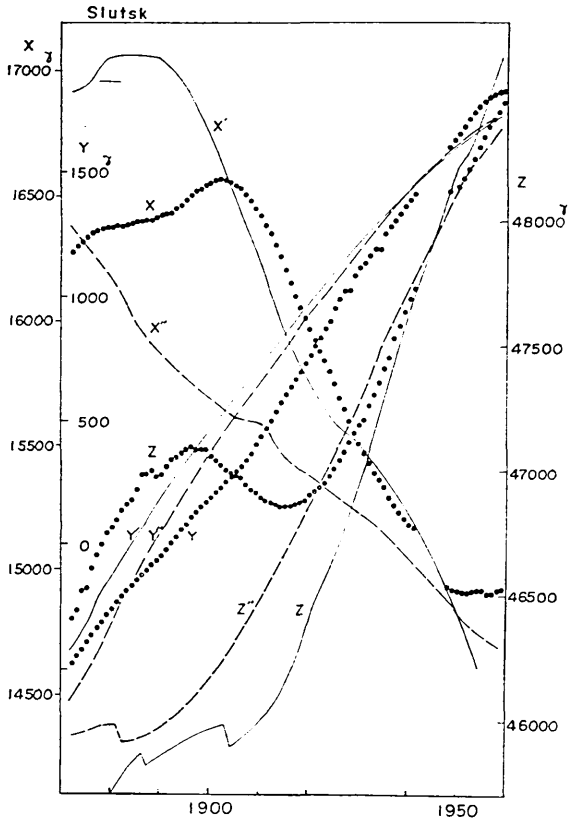

Fig. 3–4(a). Slutsk

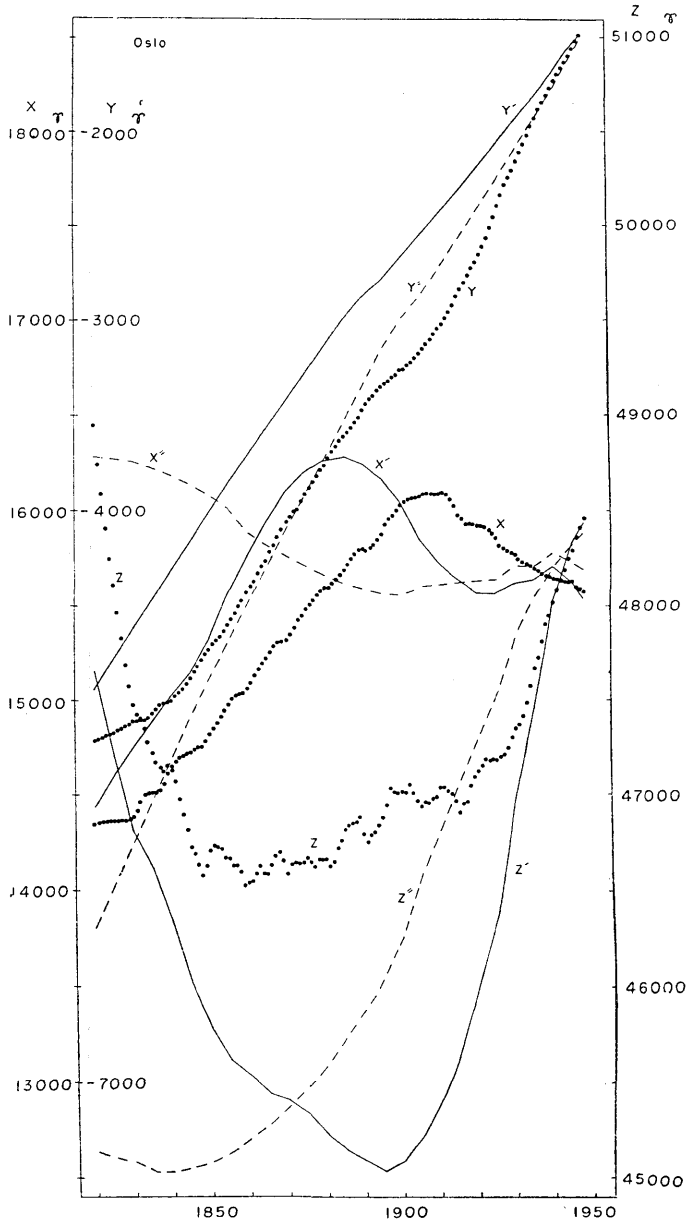
Oslo
X γ
Y γ'
Z γ
18000
17000
16000
15000
14000
13000
-2000
-3000
-4000
-7000
51000
50000
49000
48000
47000
46000
45000
1850
1900
1950
Y''
Y'
Y
X''
X'
X
Z
Z
Z''
Z'

Fig. 3-4(b). Oslo

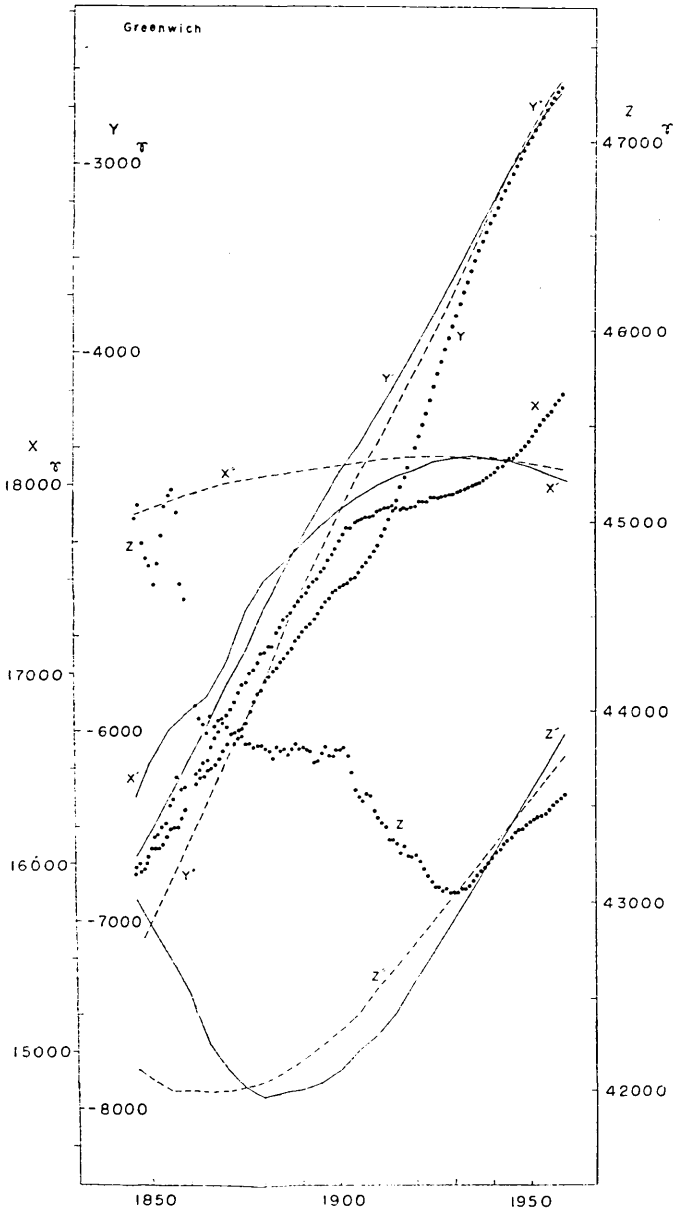

Fig. 3-4(c). Greenwich

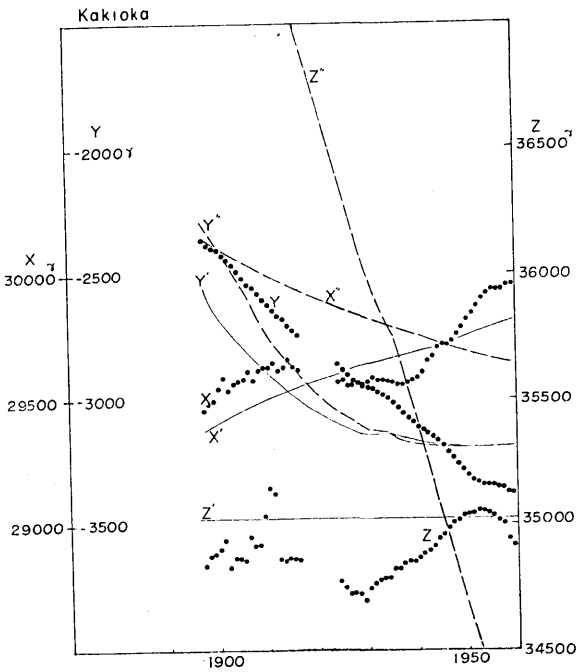

Fig. 3-4(d). Kakioka

both for the north and vertical components. The distribution of the velocities thus obtained seems to have some relation on that of the non-dipole field (Fig. 3–8), namely, in the west part of the centre of the non-dipole field in Mongolia, the velocities determined are large, and in the east part they are small.

3–5. The growth and decay of the non-dipole field.

As for the scattering of the values of drift determined in the above, we may think of two causes; one is that the magnetic field really moves with these different velocities at each station and the other is that the changes in the field occurring in the core, which produce the residual field in the equation (1–4) are not always so small and random that they cannot be nullified by the integration over the period of observation. We cannot distinguish which is the true cause from magnetic observation alone.

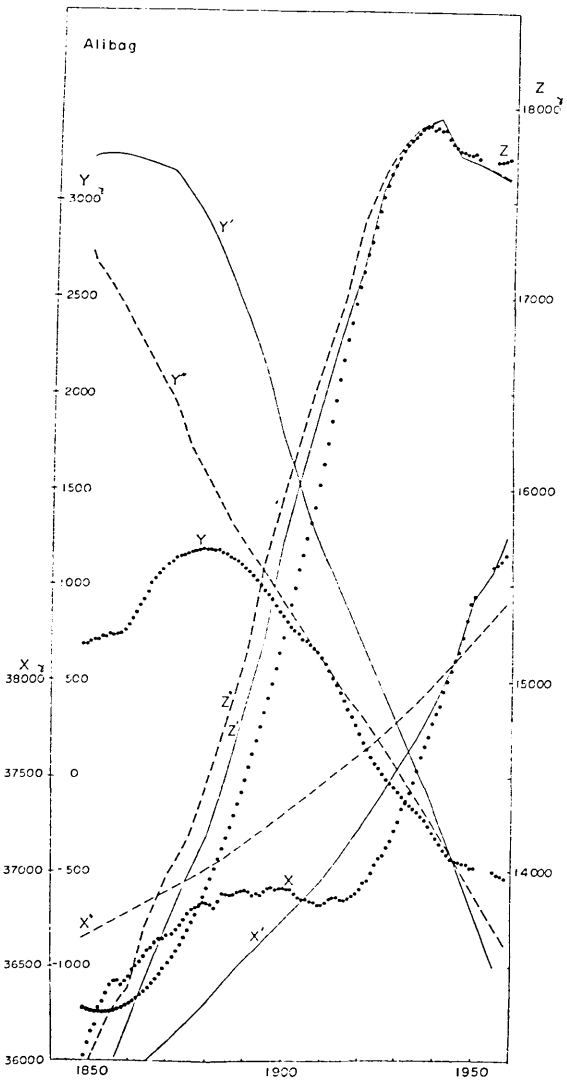

Fig. 3-4(e). Alibag

Fig. 3-4. Variation in the magnetic field at various stations. Full lines show the variations which are caused by the westward drift with the velocities determined by making $\emptyset$ a minimum. Broken lines show the variations expected when the field drifts with the mean velocity $0.20°/yr$.

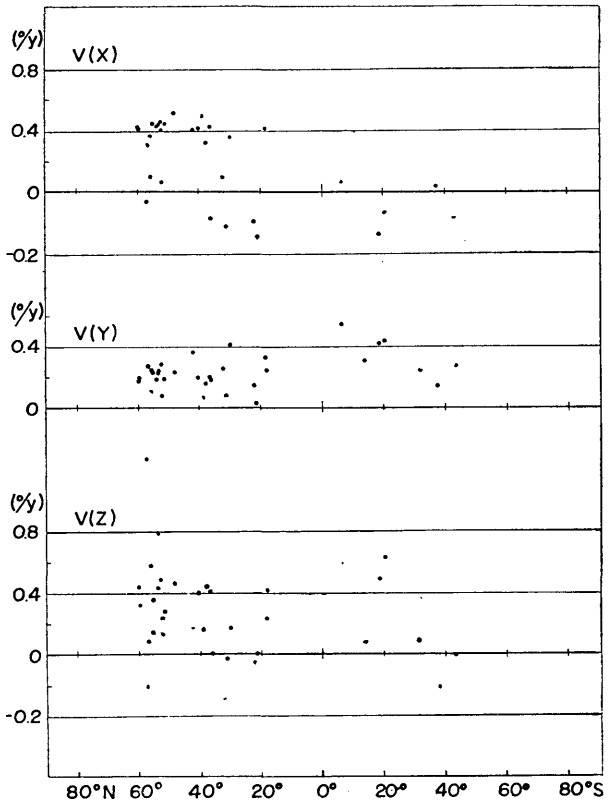

Fig. 3-5. Distributions of the velocities obtained for each component of the magnetic field.

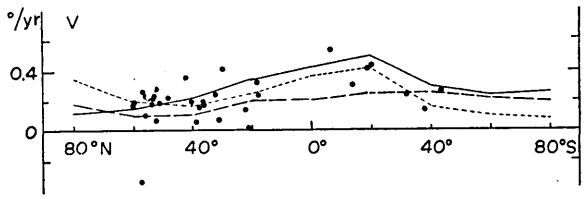

Fig. 3-6. Comparison of distribution of the velocities for Y-component with those obtained from magnetic potential.

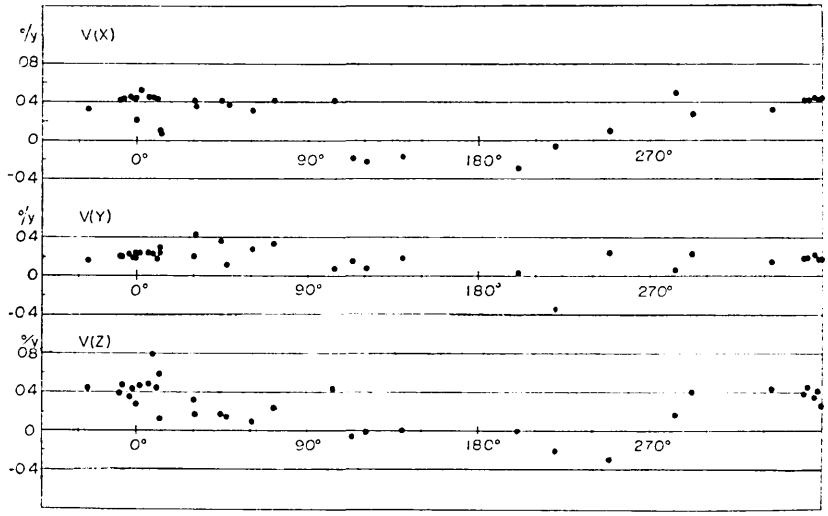

Fig. 3-7(a). Northern hemisphere

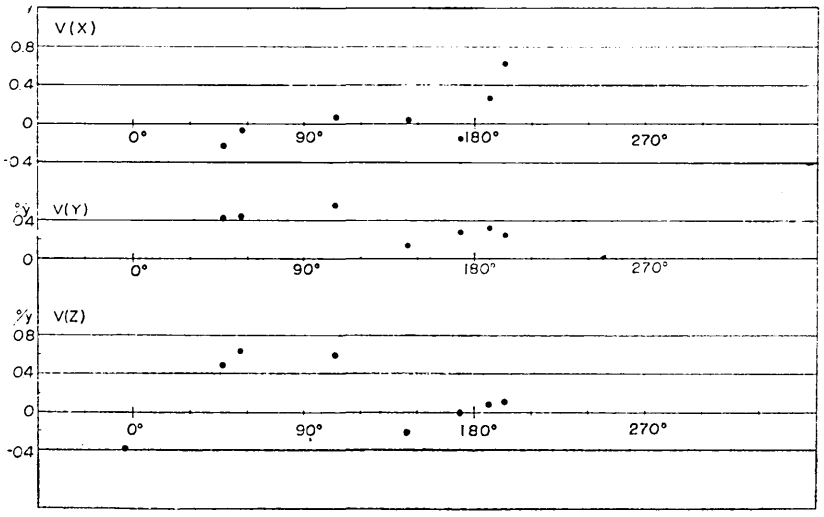

Fig. 3-7(b). Southern hemisphere

Fig. 3-7. Variation of drift velocity with longitude.

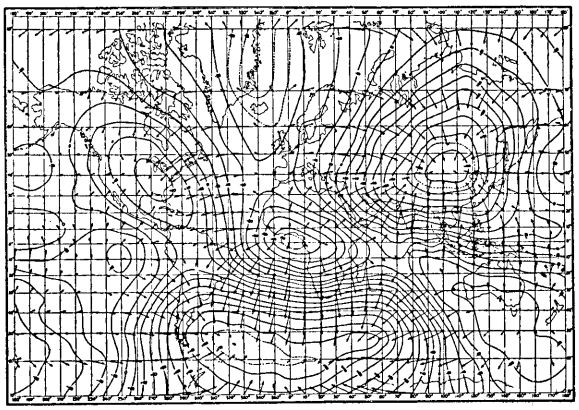

Fig. 3-8(a). Vertical component. Contour interval 0.02 gauss.

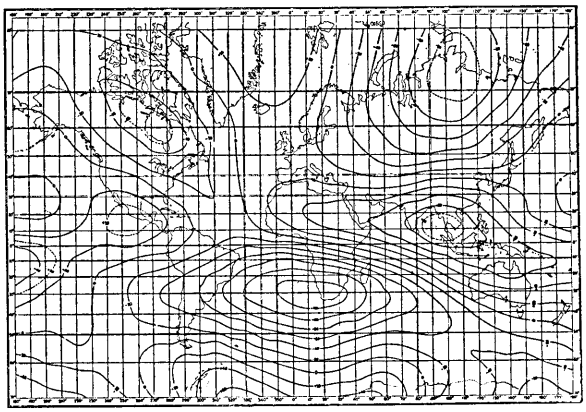

Fig. 3-8(b). North component. Contour interval 0.02 gauss.

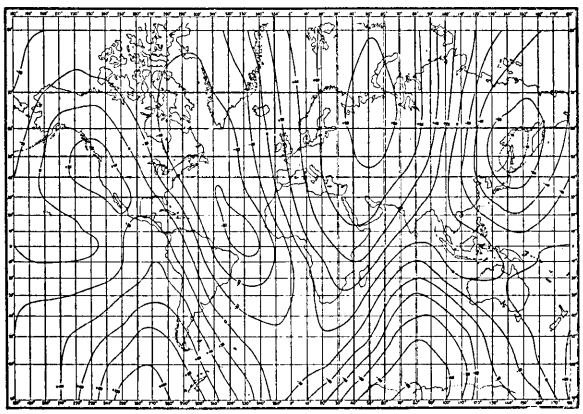

Fig. 3-8(c). East component. Contour interval 0.02 gauss.

Fig. 3-8. Non-dipole field for 1945. (After Bullard)

It is difficult to suppose, however, that each component of the magnetic field moves with velocities different from each other, as long as the magnetic field is assumed to drift together with the fluid in the top layer of the core. Moreover, the correspondence concenring the distribution of the drift velocity with that of the non-dipole field suggests that the scattered velocities may be the products of the wax and wane of the non-dipole field. When the non-dipole field changes its intensity at a place where the isodynamic lines run in an east-west direction, quite an erroneous velocity of the westward drift is obtained. It is supposed that this should be near the case for determinations from the north and the vertical components. Since isodynamic lines run north or southwards, the east component seems the most reliable for determining the westward drift velocity. Taking the accuracy of the data used into account, we are going to estimate, in the first place, the drift velocity, on the assumption that the magnetic field drifts with a constant velocity everywhere on the earth.

As is shown in Fig. 3–7, good agreements can be seen between the

Table 3–4. Local means of drift velocity (°/*yr*)

Region	V (X)	V (Y)	V (Z)
A	0.33±0.006	0.23±0.007	0.47±0.016
B	0.39±0.008	0.21±0.006	0.20±0.017
C	0.30±0.021	0.26	0.08±0.004
D	0.40±0.011	0.07±0.003	0.23±0.002
E	−0.21±0.004	0.12±0.003	−0.02±0.000
F	−0.07±0.003	−0.34±0.006	−0.22±0.011
G	0.09±0.003	0.24±0.001	−0.30±0.004
H	0.49±0.080	0.06±0.002	0.16±0.003
I	0.41±0.032	0.19±0.004	0.38±0.015
J	0.35±0.009	0.41±0.005	0.16±0.004
K	0.41±0.033	0.32±0.020	0.22±0.001
L	−0.20±0.003	0.14±0.004	−0.06±0.001
M	−0.30±0.013	0.02±0.001	0.00
N	0.27±0.006	0.23±0.002	0.41±0.048
O	−0.19±0.003	0.42±0.018	0.55±0.007
P	0.05	0.54	0.59
Q	0.26±0.008	0.30	0.07
R	0.03	0.13±0.008	−0.22±0.004
S	−0.17±0.002	0.26±0.007	−0.01±0.000
T	0.62±0.008	0.23±0.009	0.09±0.001

drift velocities computed from the data in Europe, where we have the densest distribution of observatories in the world. Such agreement may suggest that even the velocity estimated at one station can safely be regarded as representing the drift velocity of the field in a fairly wide region around the station. The world distribution of the observatories is divided with parallels and meridians at 30° intervals (Fig. 3-1). The mean velocities for each region are computed as are shown in Table 3-4. They are averaged again giving the averaged values for the whole earth. The results for the three components $V(X)$, $V(Y)$ and $V(Z)$ are

$$V(X)=0°.163\pm0°.016 \text{ per year}$$
$$V(Y)=0°.202\pm0°.006 \text{ per year}$$
$$V(Z)=0°.139\pm0°.013 \text{ per year}$$

As the velocity for the north and the vertical component seems to be much affected by the wax and wane of the non-dipole field, we shall adopt the mean velocity $0.202°/yr$ for the east component as the angular velocity with which the earth's field is rotating uniformly. The variations caused by the uniform rotation with this velocity are depicted by broken-lines in Fig. 3-3 and Fig. 3-4.

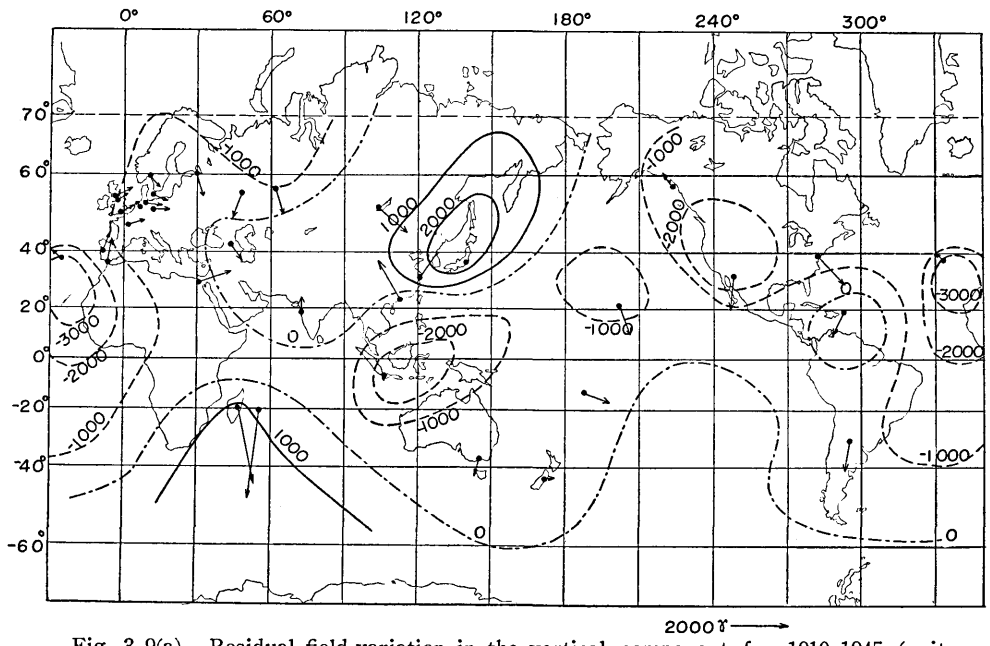

Fig. 3-9(a). Residual field-variation in the vertical component for 1910-1945 (unit in γ). Arrows represent horizontal component.

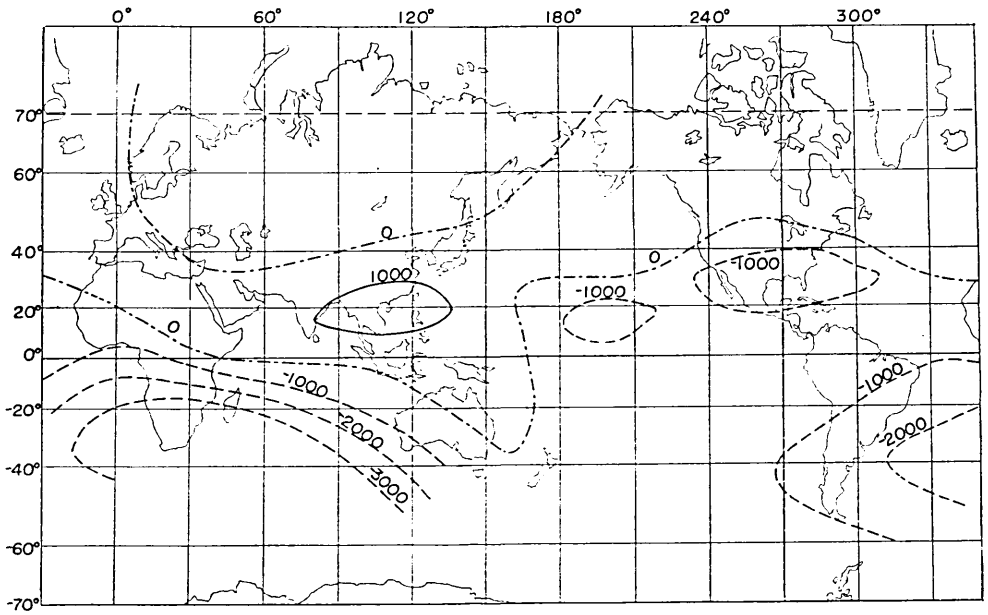

Fig. 3-9(b). Residual field-variation in the north component for 1910-1945 (unit in γ).

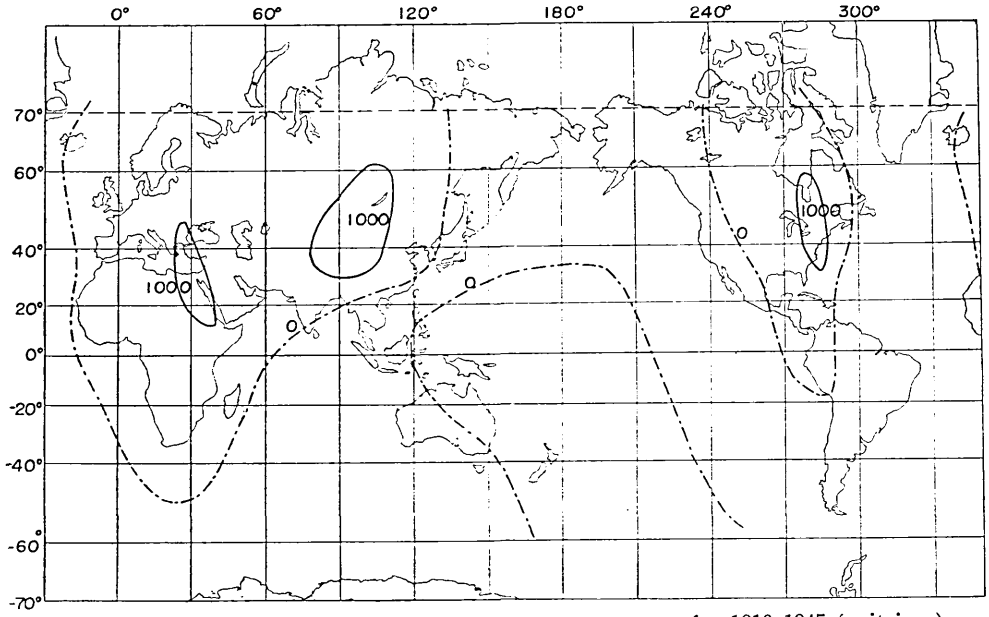

Fig. 3-9(c). Residual field-variation in the east component for 1910-1945 (unit in γ).

By making use of this uniform velocity, the changes in the residual field from 1910 to 1945 are calculated and shown in Fig. 3-9. Comparing it with the maps of the non-dipole field in Fig. 3-8, it may be noticed that the lines of no variation agree well with the nodal lines of the non-dipole field. This means that the foci of the non-dipole field are changing in intensity. Fig. 3-9 shows that the maximum of the vertical component in South Mongolia and the minimum in Africa are becoming more pronounced and that the maximum in North America is decaying.

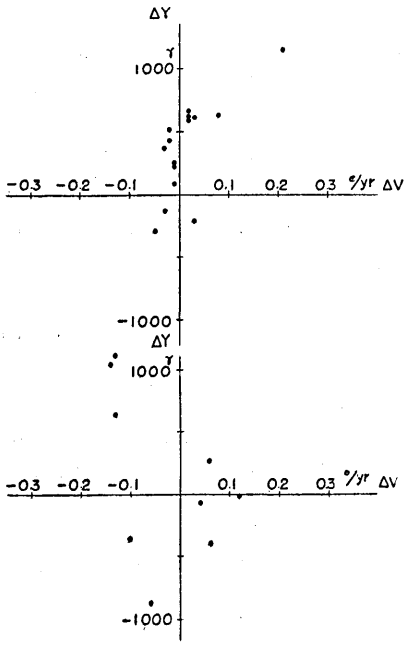

Fig. 3-10. Relations between the deviation of the apparent velocity from the mean (Δv) and the residual field variation (ΔY) regarding the stations on the ascending side (top diagram) and descending side (bottom diagram) of the non-dipole field.

Relations between the deviation of the apparent velocity from the mean and the residual field variation, after subtracting the contribution of the uniform drift, are briefly examined with respect to the east component. Correlation between them is shown in Fig. 3-10 regarding the observatories

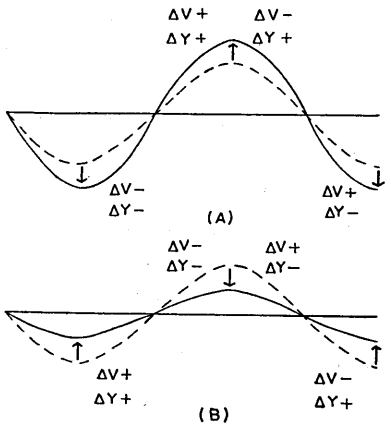

Fig. 3-11.

in Europe and Asia on the ascending side from the minimum to the maximum or on the descending side from the maximum to the minimum of the non-dipole field. Positive correlation can be seen on the ascending region, while negative correlation seems to exist on the descending part. This can be explained clearly by the intensification of the hill and dale of the non-dipole field. Relations between the deviation of the field and the residual field are

schematically shown in Fig. 3-11 in two typical cases in which the hill and dale are growing or they are decaying. The result shown in Fig. 3-10 is the former case.

3-6. Contribution of the westward drift to the observed rate of change in the field.

Isoporic charts for 1955-60 by Nagata and Syono[24] are shown in Fig. 3-12. Strong increase in the vertical intensity is seen in Turkey and in the South polar region. The centres of negative sign exist in the Indian Ocean and in the Atlantic Ocean. These strong increases or decreases in the field are greatly reduced in the charts of the residual field variation during the 35 years dealt with in Fig. 3-9. Especially for the east component, the maximum of the residual variation over 35 years is 1154γ, namely a little less than $33\gamma/year$, while the isoporic chart in Fig. 3-9 gives a rate of $70\gamma/year$. From these it may be said that the greater part of the observed rate of change is caused by the westward drift of the non-dipole field.

As is shown in Fig. 3-4 the magnetic field sometimes changes within the short period of a decade or so, superposing on the general slow variation. Short period variation are emphasized in the diagrams of the rate of change as in Fig. 3-3. Though they have large amplitudes in the rate of change, they are of little significance when averaged over long periods. In order to eliminate fluctuations of short period, the rate of change observed should be averaged over a long period. These averaged variations will shed light on the question what a great part the drifting field plays in the observed secular variation.

Where the isodynamic lines of the non-dipole field run exactly in the east-west direction, no time variation would be observed by the westerly rotation of the field alone. In most parts of the world, the magnetic field is distributed with some gradient, east- or westward, though isodynamic lines of the non-dipole field run in the east-west direction at some areas. (In the latter cases, the westward drift cannot be detected.) The contribution of the westward drift to the observed secular variation should not be ignored. The most favourable places for the westward drift to be determined accurately are where the magnetic fields vary east- or westwards with a steep gradient. In these places the variations which may be expected from the uniform drift of

24) T. NAGATA and Y. SYONO, *loc. cit.*, 15).

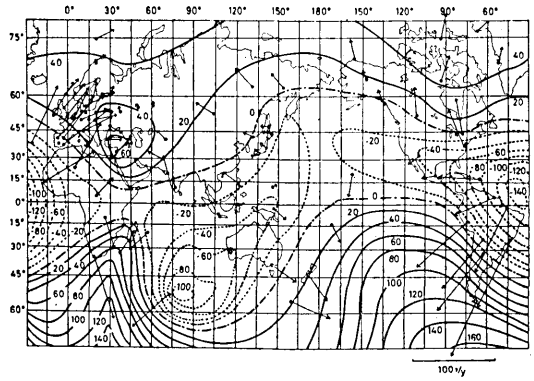

Fig. 3-12(a). Vertical component

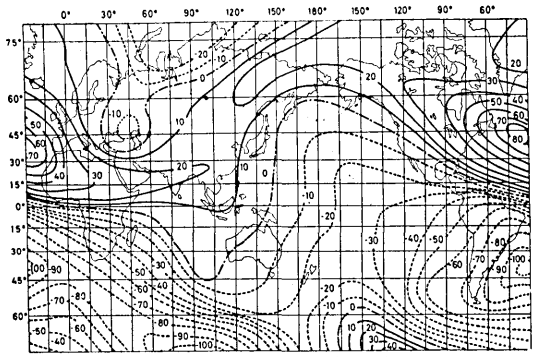

Fig. 3-12(b). North component

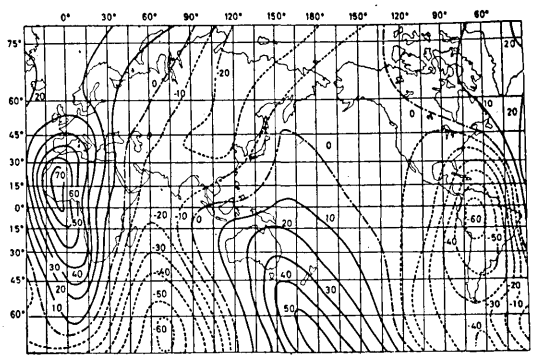

Fig. 3-12(c). East component

Fig. 3-12. Isoporic charts for 1955-1960 (unit in γ/yr) (after Nagata and Syono)

the field are compared with the observation. The rates of change due to the drift are averaged during the period of observation and are shown in Table 3–5 together with those in the observed field concerning

Table 3–5. Examples of the mean rates of change in the field observed and those expected from the westward drift

Observatory	Component	Period (yr)	Mean rates of observed variation (γ/yr)	Mean rates of change by the drift (γ/yr)
Slutsk	X	82	−17.2	−18.6
Slutsk	Y	82	27.0	26.9
Slutsk	Z	82	22.9	29.3
Oslo	Y	95	33.4	35.1
Oslo	Z	95	17.5	32.5
Greenwich	Y	88	39.5	41.0
Dusheti	Z	75	52.5	66.9
Coimbra	Y	88	38.6	41.0
Kakioka	Y	56	−17.0	−14.5
Alibag	X	105	23.2	15.8
Alibag	Z	105	42.5	43.7
Toolangi	Y	58	7.7	13.6

the several selected features of the magnetic field. Quite good agreements can be seen between them. For example, the north component at Slutsk has varied with the mean rate of change $-17.2\gamma/yr$ for the past 82 years, while the rotation of the field should have produced the variation in the field there at the mean rate of $-18.6\gamma/yr$ during the same period. It may be concluded, therefore, that the westward drift of the non-dipole field occupies almost all the time variation in the field.

3–7. Concluding remarks.

It has been well established that the magnetic field at an observatory changes conspicuously within the short period of several decades or so, while the variation due to the westward drift of the non-dipole field, as is supposed from its velocity, is expected to take place very slowly with a time scale of several hundred years, on condition that the non-dipole field survives long enough. Although a number of investiagators have excluded the possibility of accounting for the field changes by the westward drift, because of the short life-time of the non-dipole field,

the analyses conducted in this chapter prove that the westward drift is a very important factor in the secular changes observed at observatories. This in turn suggests that the life-time of the non-dipole field must be fairly long.

The velocities obtained by correlating the observation to the expected variation due to the drift are widely scattered in the cases of the north and the vertical components, while those for the east component show good agreements. This seems likely to be associated closely with the distribution of the observatories. The westward drift has no effect at places where no variation in the non-dipole field is seen along parallels of latitude. A large number of the stations utilized are distributed in the middle latitude where the isodynamic lines for the north component run nearly parallel to the latitude. Meanwhile the lines for the east component tend to run in a meridian. Consequently, the analysis of the east component is the most reliable in the determination of the drift velocity. The velocity thus obtained from the east component, $0.202°/yr$ say, agrees with those calculated from the results of harmonic analyses.

When the variation due to the drift is subtracted from the one actually observed, the rate of change in the field is markedly reduced. The maps of the rate of change become simple after the subtraction in contrast to the rather complicated distribution in the originals. It is also made clear that the main features of the magnetic records at a station can well be satisfactorily illustrated by the westward drift of the non-dipole field. In the favourable cases where the field changes with a steep gradient eastwards, it is assured that most of the observed rate of change is caused by the westward drift. It is therefore concluded that the westward drift of the non-dipole field occupies the largest part of the observed time variation in the field.

Chapter 4. The Variation of the Magnetic Field in Historical and Geological Times.

4–1. Introduction.

It is interesting to examine whether the variation of the historical or the geological time scale can also be explained by the westward drift of the magnetic field. If we know the spatial distribution of the magnetic field in the past, we may repeat the same procedure as that outlined in the previous chapter, and obtain the drift velocity at that time. As we have no means, however, of accurate reference to old maps

of the field beyond a hundred years, the available distribution of the field is confined to recent times. If the magnetic field had not changed its form significantly over historical time, it would be allowable to apply the previous method to the variation of the historical time scale. The non-dipole field, however, has been regarded as having been produced by the turbulent motion near the surface of the core and supposed to disappear within a hundred years or so. If this be true, our method is limited only within a hundred years. In the case of our method being applied beyond the life time of the non-dipole field, greatly scattered velocities will be obtained at every trial. Therefore it is worth while to examine the period during which our method is applicable, in order to presume the life time of the non-dipole field.

4–2. The variation in historical time.

In order to infer the variation in the past when we have no instrumental observation, the palaeomagnetic study is the only possible method to use. Our method, however, requires that the data should be continuous over a period of several hundred years. Consequently only limited sets of data are available in spite of the enormous studies in palaeomagnetism and archaeomagnetism.

The writer has inferred previously the variation in the declination and inclination in Japan from a study of rocks in Oshima Island.[25] The results are analysed here together with famous data from London and Paris where observations by instruments have been conducted since the sixteenth century. Besides these, the observational data at Oslo since 1770 are analysed.

In this chapter the observed field itself is compared with the field expected from the drift. The theoretical curves of variation are chosen so that the calculated values should take the same values as the observation at 1945. If we take a small part of variation, it is rather monotonous. Therefore it results in that the differences between the observation and the calculation increase, accordingly as time goes back from the epoch specified above. This systematic property of the differences makes the method used in this chapter irrelevant for determining the velocity, because our method is based on the assumption that the residual field varies at random. This was noticed after the calculation of this chapter was completed. On account of the extensive

25) T. YUKUTAKE, *Bull. Earthq. Res. Inst.*, **39** (1961), 467.

computation, no calculations were done over again. However, the analyses for the long period, as in this chapter, will reduce the irrelevance because both signs of the differences appear with equal frequency.

When the field patterns move westwards, the magnetic field observed at ϕ_0 can be written in the following form,

$$X(t,\phi_0)=A_0+\sum_{k=1} A_k \cos k\{v(t-t_0)+\phi_0\}+\sum_{k=1} B_k \sin k\{v(t-t_0)+\phi_0\} \qquad (4\text{–}1)$$

If we know the field distribution at $t=t_0$ along a circle of latitude, we have

$$X(t_0,\phi)=A_0+\sum_{k} A_k \cos k\phi+\sum_{k} B_k \sin k\phi,$$

and the constants A_k, B_k are determined.

In place of the equations (1–4) and (1–5), the following Φ is defined,

$$\Phi=\frac{1}{T}\sum_{k=1}^{T}[X'(t_k)-X(t_k,\phi_0)]^2 \qquad (4\text{–}2)$$

where $X'(t_k)$ is the observed field at $t=t_k$. Let an approximate velocity be v_0, then the true velocity is

$$v=v_0+\Delta v.$$

Substituting this into equation (4–2), Δv which makes the function Φ a minimum, is obtained as follows.

$$\Delta v=\frac{\sum_i \delta X_i u_i}{\sum_i u_i^2} \qquad (4\text{–}3)$$

where

$$\delta X_i=X'(t_i)-X(t_i,\phi_0)$$

$$u_i=\frac{\partial X(t_i,\phi_0,v)}{\partial v}$$

$$=(t_i-t_0)[-\sum A_k k\cos k\{v_0(t-t_0)+\phi_0\}+\sum B_k k\cos k\{v(t-t_0)+\phi_0\}]$$

In the actual calculation, taking the newly obtained velocity $v=v_0+\Delta v$ as a better approximation, the same procedures are repeated till Δv becomes less than 10^{-5} *rad./yr.*

The standard deviation of the velocity was calculated by the same type of equation (3–7), *i. e.*

$$\sigma^2=\frac{v^2}{T}\sum_{k=1}^{T}\left[\frac{1}{\frac{\partial X(t_k)}{\partial t}}\cdot\frac{\delta X(t_k)}{t_k-t_0}\right]^2 \tag{4-4}$$

The data obtained from the study of rocks in Oshima Island are shown in Fig. 4–1. The inferred variations which are reduced to those in Tokyo are shown by solid curves. Field values were read at an interval of 50 years. As to Paris and London, they are taken at intervals of 10 and 20 year respectively, and at a 2 year interval for Oslo. The calculated velocities and the probable errors are shown in Table 4–1. Except for Oslo, good agreements are seen between the drift velocities. The field variations that should be caused by the drift of the magnetic field with these velocities are shown in Fig. 4–2 by dotted lines together with the observed data. It seems likely that the drifting effect of the field has been in existence over a period of more than several hundred years.

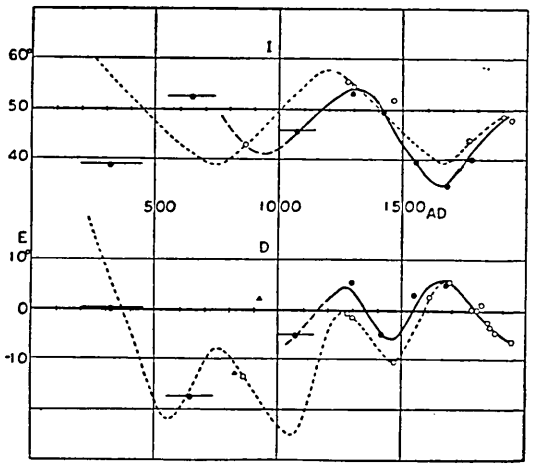

Fig. 4-1. Variation in declination and inclination with time in Japan. The upper diagram shows the variation in inclination and the lower in declination.
Solid curves were obtained from the archaeomagnetic study of rocks in Oshima. Dotted curves are the variation inferred by N. Watanabe.

At such a high latitude as Oslo, the horizontal component of the magnetic field is so small that even a slight fluctuation in its intensity

Table 4–1. Velocity of the westward drift during historical time

Observatory	Drift velocity of declination (°/yr)	Drift velocity of inclination (°/yr)
Oslo	0.64	0.66±1.20
London	0.41±0.03	0.41±0.22
Paris	0.42±0.41	0.45±0.09
Tokyo	0.39±0.01	0.37±0.02

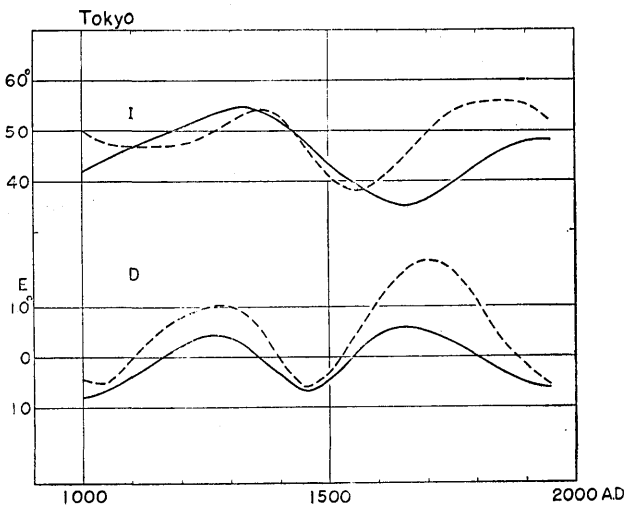

Fig. 4-2(a). Comparison of the variations in the field calculated with those observed at Tokyo. Solid curves represent observed variation. Dotted curves are the variation calculated.

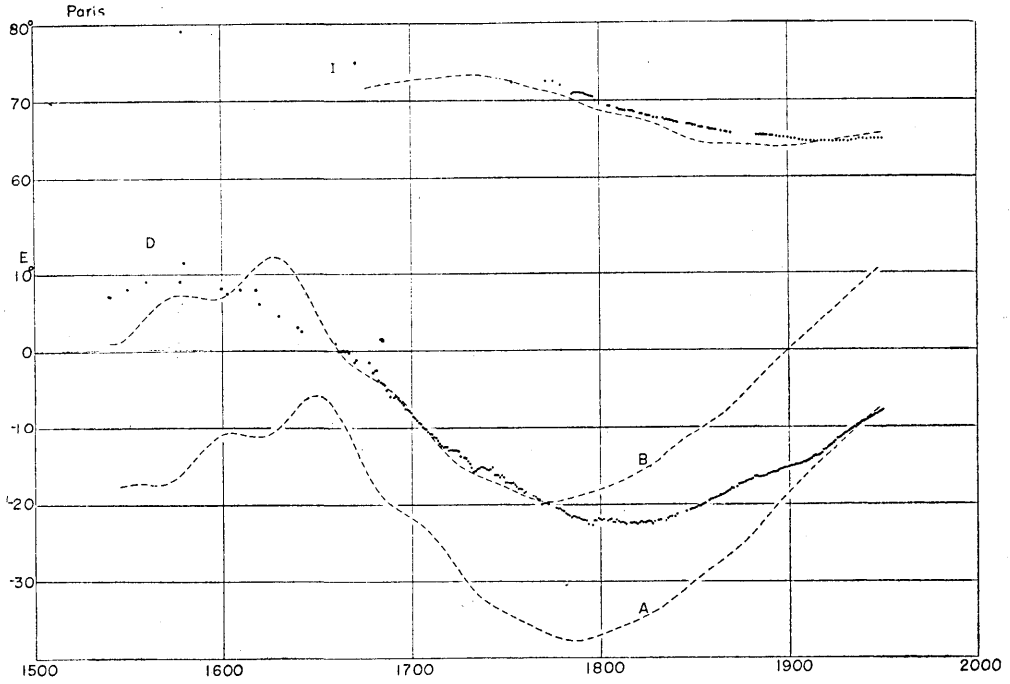

Fig. 4-2(b). Variations at Paris
Full circles represent the observed values, while dotted curves represent the calculated variations.
Curve A is the variation so that the calculated values in 1945 may become equal to those of observation. Curve B is the variation when an arbitrary constant is added in order to fit the calculation better to the observation in the past.

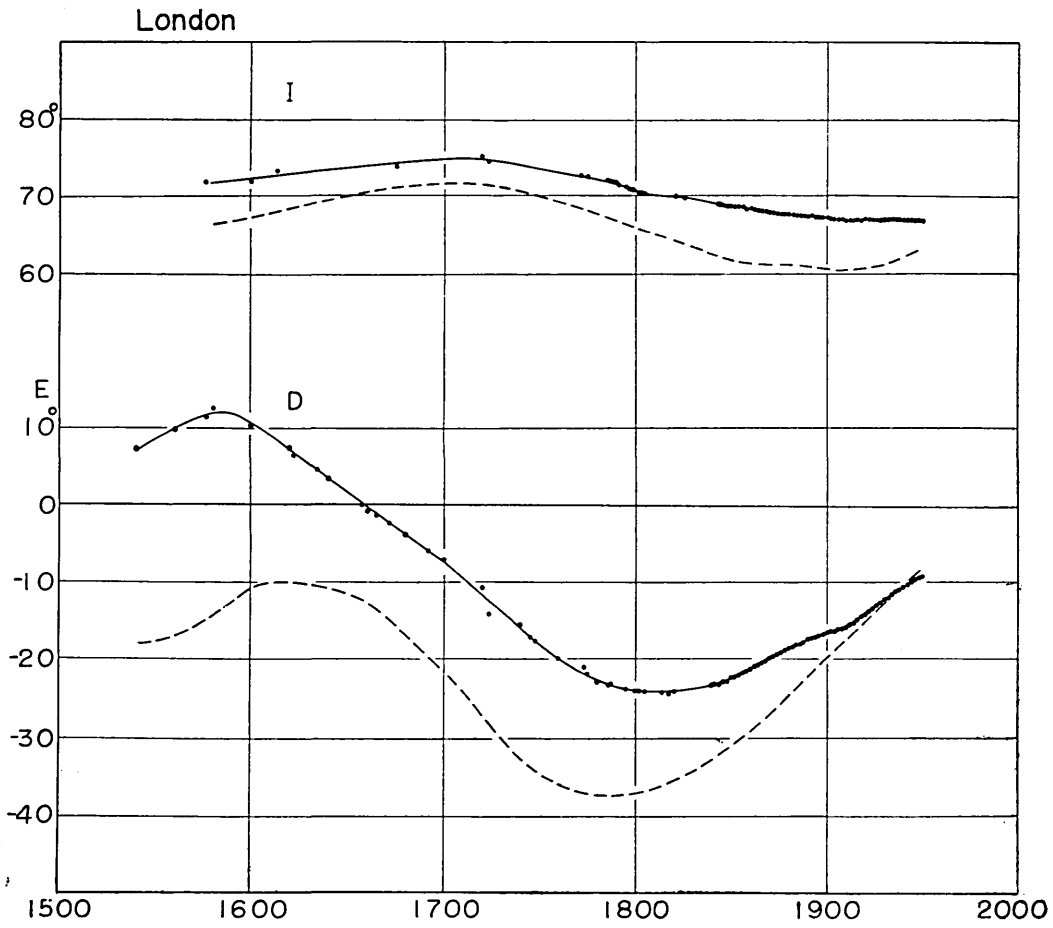

Fig. 4-2(c). At London. Dotted curves are the calculated variation

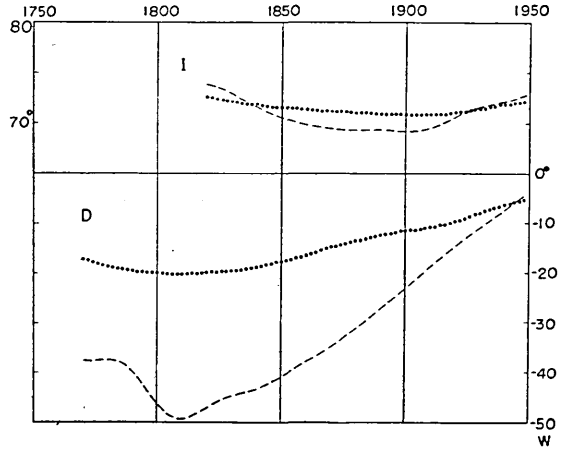

Fig. 4-2(d). At Oslo

will produce a remarkable variation in the direction of the field. This may be the reason why the extraordinarily large velocities were obtained at Oslo.

The drift velocity obtained in this chapter is about twice as large as the velocity for the analyses of recent data. It is apparent that the velocity estimated by this method is a mean during the period of integration. Therefore it seems to suggest that the magnetic field might have moved at a faster velocity in the past than at present. Another conclusion that may be derived from this study is that the present field may be taken as an approximate distribution of the field in the past, as far as these hundreds of years are concerned. Therefore the main features of the non-dipole field at present seem to have been persisting for a thousand years or so.

4–3. Spectral analyses of palaeomagnetic data.

Accordingly as the magnetic field rotates, hills and dales of the non-dipole field cause a variation as if the magnetic field varies periodically. Periodical changes appearing in archaeomagnetic study of Oshima

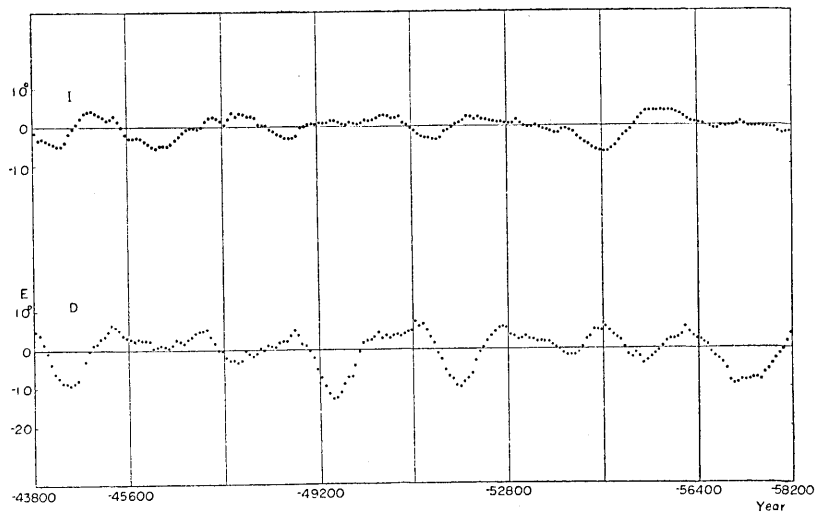

Fig. 4-3. Variation in inclination and declination with time inferred from the study of Narita bed.

Island or in historical data at London and Paris belong to this type of variation. If the main features of the field should survive beyond the period of one revolution, we could see marked periodical variation at

every rotation. Spectral analyses of palaeomagnetic data are carried out in this section.

Nagata and others[26),27),28)] studied the magnetization of a sedimentary layer, called the Narita bed, continuously from the top to the bottom. Absolute dating was made by means of the U-Ra method. Variations in the declination and the inclination with time are shown in Fig. 4–3, in which the gradual changes calculated by taking running-means are subtracted from the original data. Periodical changes are conspicuous. Fourier analyses for declination and inclination were carried out, and the amplitude for each component was calculated. Fig. 4–4a shows the results. We can see the periods of 700, 1200, 1800, and 7000 years are predominating. Similarly the periods of about 1000, 2000 and 3000 years are seen for the inclination. It seems to be common understanding, however, that the data for the inclination seem less reliable because they are inclined to suffer such disturbances as the rotation of the particles while the sedimentation is underway.

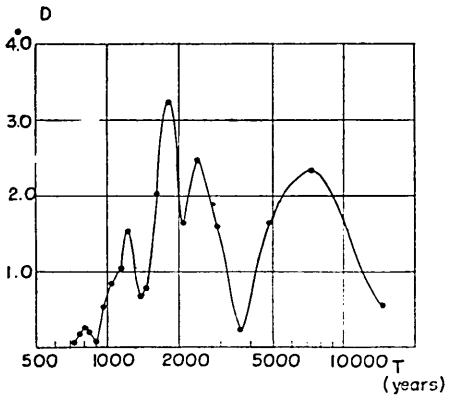

Fig. 4-4(a). Spectral analyses of variation in declination.

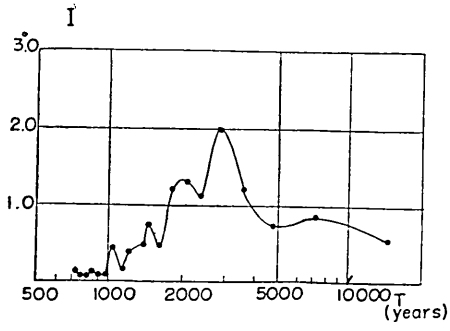

Fig. 4-4(b). Spectral analyses of variation in inclination.

There are two causes that should be taken into account for discussion on the periodicity of the field variation at one place. One is the oscillation of the earth's field and another is the rotation of a wave-like field. As Cox[29)] has pointed out, if all patterns of the field, the dipole field and the non-dipole field alike, oscillate at the same rate, no variation in the direction of the magnetic field will be observed. Even in the case where simple harmonic oscillations

26) T. NAGATA, T. RIKITAKE and K. AKASI, *Bull. Earthq. Res. Inst.*, **21**, (1943), 276.
27) T. NAGATA, Y. HARADA and K. HIRAO, *Bull. Earthq. Res. Inst.*, **23** (1945), 79.
28) T. NAGATA, K. HIRAO and H. YOSHIKAWA, *Jour. Geomag. Geoele., Kyoto.*, **1** (1949) 52.
29) A. COX, *Jour. Geomag. Geoele., Kyoto*, **13** (1962), in the press.

with different periods of the two components of the magnetic field are taking place locally, the spectra for the direction of the field may perhaps not be so simple as to be expressed by a few predominant periods. Therefore it seems more probable to regard the periodicity as the products of the rotating field.

As has been already seen, the periods of 700–800 years are likely to be closely associated with the distribution of the hills and dales of the field. The distance between the adjacent hills, however, seems too short to be related to the periods of 1200 years and 1800 years. If we assume that these periods are those of a full rotation of the field, the mean velocities of rotation are calculated as $0.3°/yr$, $0.2°/yr$ and $0.06°/yr$ corresponding to the periods of 1200 years, 1800 years and 7000 years. The velocities $0.3°/yr$ and $0.2°/yr$ agree well with the results obtained previously. This seems to suggest the possibility that the main features of the field are still preserved beyond a full rotation. It is interesting that $0.06°/yr$ is the same order of magnitude as the probable velocity of the equatorial dipole obtained by Bullard.

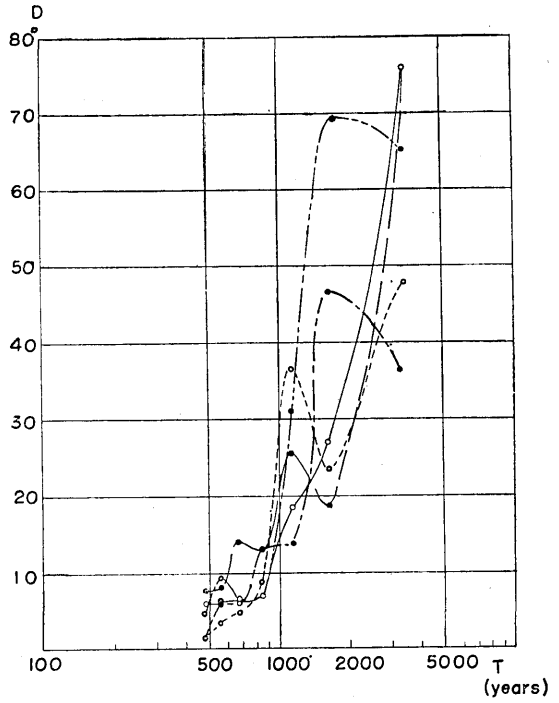

Fig. 4-5. Spectral analyses for declination of Narita bed.

It may be a point of discussion whether the different velocities of $0.3°/yr$ and $0.2°/yr$ existed at the same time or not. If they had been coexisting, two different kinds of field should have drifted independently. The whole period of the sedimentation of the Narita bed is divided into five intervals and Fourier analyses were carried out for every interval. As is shown in Fig. 4–5, either of the velocities $0.3°/yr$ or $0.2°/yr$ appears for each interval. These results are full of suggestions that the field might have rotated with the velocity

of $0.3°/yr$ during a certain period and for another period with the different velocity $0.2°/yr$, when we recollect that the mean velocity during the past several hundred years is about $0.4°/yr$ and that of several decades is $0.20°/yr$.

Johnson, Murphy and Torreson's data[30] obtained from the varves in New England were also analysed in the same way. The results are shown in Fig. 4-6. In these cases too, marked large amplitudes are

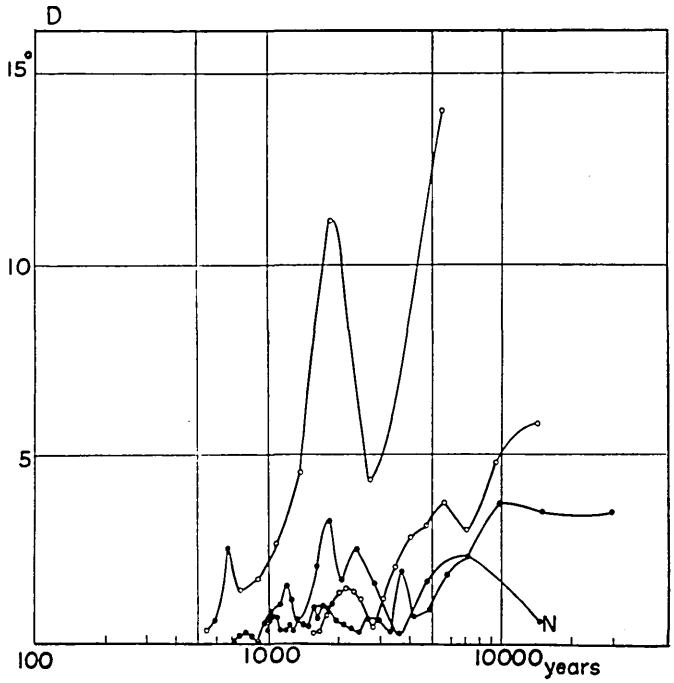

Fig. 4-6. Spectral analyses for declination of varves in New England. N is the spectrum of Narita bed.

seen at the perids of 700 years and 1800 years.

From these studies, there is some possibility that the main characteristics of the field seem to remain intact after one cycle of rotation.

Chapter 5. Summary and Conclusion.

The velocities of the westward drift of the earth's magnetic field are estimated by making use of a number of different methods. The

30) E. A. JOHSON, T. MURPHY and O. W. TORRESON, *Terr. Mag.*, **53** (1948), 349.

analyses of the magnetic potentials have given the mean volocities along circles of latitude. On the other hand, the observed variation at one station enables us to calculate the most probable velocity there during the period of observation. The velocities thus obtained on the basis of the different methods have shown good agreement mutually. On an average all through the world, a mean velocity amounting to $0.202°/yr$ is obtained. If we consider that the non-dipole parts of the earth's field drift westwards with this velocity, the main parts of the variation observed at most observatories are well accounted for by the drift of the field. The mean rates of change in the field during the period of observation are compared at some stations with those expected from the drift of the field. The agreement seems to be satisfactory. After the effect of the westward drift is subtracted from the observation, the residual fields that represent the wax and wane of the non-dipole field are calculated. The rate of growth or decay of the non-dipole field is unexpectedly small. The main parts of the time variation observed are likely to be caused by the westward drift of the non-dipole field.

Analyses for much longer periods are carried out by making use of the archaeomagnetic study on volcanic rocks in Oshima Island and the historic data at London and Paris. The westward drift of the magnetic field having a distribution which is the same as that at present seems to cause the main parts of the variation, if we take a drift velocity of about $0.4°/yr$. These results suggest that the non-dipole field had been fairly stable for the period considered. Even the analyses of the data from the Narita bed and varves in New England seem to support this too.

Summarizing all the results in this chapter, the non-dipole parts of the earth's field are likely to preserve the same form more than several hundred years. It is also highly likely that the variation caused by their drift occupies a large part of the secular variation observed. The stability of this type of field may suggest that the origin of the non-dipole field lies not only in small scale turbulence near the core boundary but also in a larger scale motion of fluid originating from a somewhat deeper part of the core.

Acknowledgments

The writer would like to express his sincere gratitude to Prof. T. Rikitake, who has given him constant support and advice in the course

of the study. His thanks are also due to Prof. T. Nagata, who has kindly permitted the writer to make use of his unpublished collection of data. He thanks Dr. S. Akimoto and Dr. S. Uyeda for their encouragement, and to Dr. K. Aki, Mr. T. Matsuno and Mr. Y. Syono for their valuable discussion in various problems.

Most of the numerical calculations were carried out by making use of electronic computers; TAC in the Engineering Research Institute, The University of Tokyo, and another computer. The writer would like to express his thanks to Dr. Miyama and others who aided the writer in using the computers.

The writer also thanks Mr. T. Yabu and Miss T. Akasegawa for their help in preparing the manuscripts.

---

1. 地球磁場の西方移動

東京大学大学院
地球物理学課程 行武毅

地磁気永年変化中，地球磁場への西方移動によつてひきおこされる変化と，磁場の消長に伴う変化とを分離する目的でこの研究はなされた．

第1章　磁場が地球核と共に，中間層に対して相対的に西へ移動する場合，地表で観測される磁場の変化中には，流体運動の変化等による磁場の成長衰退のほかに，空間的に起伏のある磁場が全体として移動することによつて生ずる変化が含まれる．もし西方移動速度の空間的時間的特性が十分詳しく知れていれば，この二種類の性質の異る変化を分離することが可能である．実際には，西方移動速度に関する我々の知識は十分とはいい難いから，まず移動速度を詳しく求めることを試みた．

最初に，観測された変化は大部分磁場の移動によると仮定して，ある時の磁場の分布が移動したためにおこる磁場の変化がもつともよく観測結果を説明できるよう移動速度を求める．違つた資料，異る方法によつて得られた移動速度が，互いに矛盾がなく，その上物理的に受容可能なものであれば，最初の仮定―観測された磁場の変化は主として磁場の移動による―は正当化されると見て差し支えない．実際に移動速度を求める方法としては，ある空間的領域内で，観測と期待値とを比較するやり方と，ある時間間隔内で比較する方法とがある．

第2章　地球磁場に関する球函数分析の結果を用いて，種々の緯度での西方移動速度を求めた．第一の方法は，磁場の分布をある緯度圏に沿つて Fourier 級数で表現し，各項の位相の進み遅れを時間とともに追うことである．第二の方法は第1章で述べた方法（空間的な平均法）で，磁場自体とその変化率との解析結果を組み合わせて速度を求めるやり方である．この二種類の方法で得られた結果はきわめてよく一致する．

解析をおこなつた結果 $m=1$ で表現される磁場は，異つた速度で移動する種類の磁場から構成される．約 $0.06°/yr$ で移動する赤道面双極子と，他の $0.2°/yr$ の速度をもつ非双極子磁場とである．この両者は移動速度が明らかに異ることから発生機構も違つたものだと推定される．$m=2$ に関する西方移動速度は南半球で急激に増大する．$m=3$ については，北半球の高緯度地方で東向きの移動が

みられる．各項の振幅分布を考慮すると，磁場全体の移動は主として $m=1$ の項によつて支配され，上述の特異性は現われない．

第3章　50年以上の連続観測をおこなつている 34 ヶ所の観測所の観測結果と，1945年の非双極子磁場の分布とから，第1章で述べた時間的平均法によつて移動速度を求めた．X 成分，Z 成分について得られた値はばらつくが，Y 成分に関して得られた速度分布は第2章で得られた結果とよく一致する．今磁場が世界中一様な速度で移動するとして，Y 成分について得られた値を平均すると，$0.202°/yr$ の速度が得られる．この平均速度で磁場が移動した場合に期待される変化を計算して観測値との差をとると，通常観測される変化に比べて著しく小さなものとなる．これは観測される磁場の変化の大部分が，磁場の西方移動によつて生じていることを意味している．上述の観測値と計算値の差の空間的分布は，非双極子磁場の成長衰退の様子を示している．

第4章　岩石磁気学的方法によつて得られた日本における約 1000 年間の偏角，伏角の変化，16世紀以来のパリとロンドンにおける観測，および最近のオスロにおける偏角伏角の変化と 1945 年の磁場の分布とを用い，前章と同種の解析をおこなつた．約 $0.4°/yr$ の速度で西方移動したとすれば，日本，パリ，ロンドンの磁場の変化をよく説明できる．現在と過去とで移動速度が違つていたのではないかと推定される．また 1945 年の磁場の分布を数百年の過去にさかのぼつて適用できるということは，非双極子磁場がこの間安定に存在していたことを意味している．

成田層および New England の Varves についてなされた古地磁気学的研究結果を用い，偏角変化の周期分析をおこなつた．1200 年，1800 年に卓越した周期が存在する，もし磁場の回転によつてこの周期が現われたと考えると，それぞれ $0.3°/yr$，$0.2°/yr$ で回転していることになる．これは前に得られた結果とよい一致を示す．非双極子磁場の分布が長期にわたつて保たれることを暗示しているように思われる．

以上の研究から，観測される磁場の変化は大部分磁場の西方移動によつてひき起されること，非双極子磁場の分布が数百年間にわたつて安定に存在することが結論される．